MULTI-FLUID PROBLEMS IN MAGNETOHYDRODYNAMICS WITH APPLICATIONS TO ASTROPHYSICAL PROCESSES

by

Eric John Greenfield

A Dissertation Submitted to the Faculty of the

DEPARTMENT OF PHYSICS

In Partial Fulfillment of the Requirements
For the Degree of

DOCTOR OF PHILOSOPHY

In the Graduate College

THE UNIVERSITY OF ARIZONA

2015

THE UNIVERSITY OF ARIZONA
GRADUATE COLLEGE

As members of the Dissertation Committee, we certify that we have read the dissertation prepared by Eric John Greenfield
entitled Multi-Fluid Problems in Magnetohydrodynamics with Applications to Astrophysical Processes
and recommend that it be accepted as fulfilling the dissertation requirement for the Degree of Doctor of Philosophy.

Joe Giacalone — Date: 8 December 2015

Michael Shupe — Date: 8 December 2015

Brian Leroy — Date: 8 December 2015

Koen Visscher — Date: 8 December 2015

Final approval and acceptance of this dissertation is contingent upon the candidate's submission of the final copies of the dissertation to the Graduate College.
I hereby certify that I have read this dissertation prepared under my direction and recommend that it be accepted as fulfilling the dissertation requirement.

Dissertation Director: J. R. Jokipii — Date: 8 December 2015

STATEMENT BY AUTHOR

This dissertation has been submitted in partial fulfillment of requirements for an advanced degree at the University of Arizona and is deposited in the University Library to be made available to borrowers under rules of the Library.

Brief quotations from this dissertation are allowable without special permission, provided that accurate acknowledgment of source is made. Requests for permission for extended quotation from or reproduction of this manuscript in whole or in part may be granted by the head of the major department or the Dean of the Graduate College when in his or her judgment the proposed use of the material is in the interests of scholarship. In all other instances, however, permission must be obtained from the author.

SIGNED: Eric John Greenfield

ACKNOWLEDGEMENTS

There are many individuals and groups I would like to acknowledge and thank for their contributions during my graduate career. Their constant guidance and advice helped me finally reach this point.

First and foremost, I want to say thank you to my advisor, Randy Jokipii. Thank you for taking me on as a "probationary" student when I first arrived in Tucson and eventually promoting me to a research assistant in the Solar and Heliospheric Research Group at LPL. Over the years I have learned a great deal from you about physics and the academic way of life. Our experiences in the trials of publication taught me about the ups and downs of research.

To the rest of the group at LPL; Joe Giacalone, Jozsef Kota and Federico Fraschetti, another heartfelt thank you. The numerous discussions over the years were invaluable in helping me finish my degree. The weekly lunch meetings with the group allowed me to discuss my work among peers, but more importantly hearing about your work kept me up to date when my focus became too narrowed.

Thank you Johnny Hsieh for meeting with me during my prospective graduate visit to the University of Arizona and introducing me to Randy and Joe. Your continued optimism and encouragement was always uplifting.

Thank you to the staffs in both the Physics and Planetary Science departments. Your diligence meant I was always in the right classes, signed up for the right credits and ensured I got a paycheck every two weeks.

I also want to thank my wonderful officemates Fan Guo, Erica McEvoy and Peng Sun for the countless discussions on math and physics. Equally important were the discussions covering topics outside of our work that helped to break up the days spent behind our computer screens.

Lastly, thank you to NASA for providing the funding that made this work possible.

DEDICATION

For my amazing wife Lisa and my parents Mary Jo and John for the unwavering support that made this dissertation possible. To Owen and baby girl, I love you both more than you know.

TABLE OF CONTENTS

TABLE OF CONTENTS – *Continued*

LIST OF FIGURES

ABSTRACT

I begin this study by presenting an overview of the theory of magnetohydrodynamics and the necessary conditions to justify the fluid treatment of a plasma. Upon establishing the fluid description of a plasma we move on to a discussion of magnetohydrodynamics in both the ideal and Hall regimes. This framework is then extended to include multiple plasmas in order to consider two problems of interest in the field of theoretical space physics. The first is a study on the evolution of a partially ionized plasma, a topic with many applications in space physics. A multi-fluid approach is necessary in this case to account for the motions of an ion fluid, electron fluid and neutral atom fluid; all of which are coupled to one another by collisions and/or electromagnetic forces. The results of this study have direct application towards an open question concerning the cascade of Kolmogorov-like turbulence in the interstellar plasma which we will discuss below. The second application of multi-fluid magnetohydrodynamics that we consider in this thesis concerns the amplification of magnetic field upstream of a collisionless, parallel shock. The relevant fluids here are the ions and electrons comprising the interstellar plasma and the galactic cosmic ray ions. Previous works predict that the streaming of cosmic rays lead to an instability resulting in significant amplification of the interstellar magnetic field at supernova blastwaves. This prediction is routinely invoked to explain the acceleration of galactic cosmic rays up to energies of 10^15 eV. I will examine this phenomenon in detail using the multi-fluid framework outlined below. The purpose of this work is to first confirm the existence of an instability using a purely fluid approach with no additional approximations. If confirmed, I will determine the necessary conditions for it to operate.

CHAPTER 1

Introduction

1.1 Fluid Description of Plasma

The problem of plasma dynamics is in general a complicated one. A general solution involves knowing and keeping track of the position and momentum of every particle within the plasma. The number of degrees of freedom necessary to describe these microscopic variables alone is staggering before particle dynamics are even considered. In the kinetic theory of plasmas, this information is contained within the distribution function, $f(\mathbf{x}, \mathbf{p})$. This function evolves with time as forces alter the position and momentum of the individual particles. One method for avoiding the full kinetic theory associated with following individual particles is to instead approximate the motion of the plasma as a fluid. The collective motion of a fluid can then be described in terms of macroscopic variables such as average bulk velocity and particle number density which are calculated from $f(\mathbf{x}, \mathbf{p})$.

$$n(\mathbf{x}) = \int f(\mathbf{x}, \mathbf{p}) d^3p \tag{1.1}$$

$$\mathbf{v}(\mathbf{x}) = \int \mathbf{u}(\mathbf{p}) f(\mathbf{x}, \mathbf{p}) d^3p \tag{1.2}$$

Rather than having to keep track of the location and momentum of each particle in the plasma, the dynamics of n and $\langle \mathbf{v} \rangle$ are calculated and observed. While the small-scale motion of individual particles in lost in this macroscopic limit, much of the essential physics of the plasma is present making the fluid approach popular in

many areas of research. This method of studying the evolution of a fluid is called hydrodynamics. Below, we will review the essential equations used in hydrodynamics.

The primary equations for hydrodynamics are based upon fundamental conservation laws of physics; those of mass, momentum, and energy. By definition, as long as a quantity is conserved the time rate of change of that quantity must be equal to the negative divergence of its flux.

$$\frac{\partial A}{\partial t} + \nabla \cdot (A\langle \mathbf{u} \rangle) = 0 \tag{1.3}$$

Here, $\mathbf{u}$ is the total velocity of the particles in the plasma. This total velocity can be separated into two components, the bulk plasma velocity $\mathbf{v}$ from above and random thermal velocities $\mathbf{w}$: $\mathbf{u} = \mathbf{v} + \mathbf{w}$. Note an additional definition: $\langle \mathbf{u} \rangle = \mathbf{v}$. This implies that $\langle \mathbf{w} \rangle = 0$ which has the physical meaning that all random motions of particles within a plasma cancel with one another and do not contribute to the bulk speed of the plasma.

1.1.1 Conservation of Mass

If A is taken to be the plasma mass density nm we find the first equation for hydrodynamics which simply shows that the motion of the plasma must conserve mass (and particles), as expected. Any rate of change in the plasmas local mass density is simply due to a divergence of the mass flux.

$$\frac{\partial (nm)}{\partial t} + \nabla \cdot (nm\mathbf{v}) = 0 \tag{1.4}$$

Only the bulk velocity remains in the above equation because after averaging **u** over all of the particles in the plasma the random motions indeed cancel with one another.

1.1.2 Conservation of Momentum

In a similar manner, we now consider the conservation of momentum density in a plasma.

$$\frac{\partial \left(nm\langle \mathbf{u} \rangle\right)}{\partial t} + \nabla \cdot \left(nm\langle \mathbf{uu} \rangle\right) = 0 \tag{1.5}$$

In the equation above, the product of the two velocity vectors is an outer product not the more common inner (dot) product. The outer product between two vectors results in a tensor rather than a scaler.

$$\langle \mathbf{uu} \rangle = \begin{pmatrix} u_x u_x & u_x u_y & u_x u_z \\ u_y u_x & u_y u_y & u_y u_z \\ u_z u_x & u_z u_y & u_z u_z \end{pmatrix} = \langle u_i u_j \rangle \tag{1.6}$$

The final equality represents the tensor in the more compact index notation. Below is the entire momentum conservation equation in index notation.

$$\frac{\partial \left(nm\langle u_i \rangle\right)}{\partial t} + \frac{\partial}{\partial x_j}\left(nm\langle u_i u_j \rangle\right) = 0 \tag{1.7}$$

Recall that **u** is the total velocity of the particles within the plasma and equal to the sum of the bulk plasma speed and random thermal motions: $\mathbf{u} = \mathbf{v}+\mathbf{w}$. Inserting this definition into into equation (1.7) we find the following.

$$\frac{\partial}{\partial t}\left(nm\langle v_i + w_i\rangle\right) + \frac{\partial}{\partial x_j}\left(nm\langle v_i + w_i\rangle\langle v_j + w_j\rangle\right) = 0$$
$$\rightarrow \frac{\partial}{\partial t}\left(nm\langle v_i + w_i\rangle\right) + \frac{\partial}{\partial x_j}\left(nm\langle v_i v_j + w_i w_j + v_i w_j + v_j w_i\rangle\right) = 0 \tag{1.8}$$

Carrying out the averages in (1.8), the terms that are linear in w_i or w_j will vanish for the reasons mentioned above.

$$\frac{\partial}{\partial t}\left(nmv_i\right) + \frac{\partial}{\partial x_j}\left(nm(v_i v_j)\right) + \frac{\partial}{\partial x_j}\left(nm\langle w_i w_j\rangle\right) = 0 \tag{1.9}$$

The final term on the LHS of the equation above is recognized as the divergence of the plasma pressure tensor, $\overline{\overline{P}}$. This pressure terms appears in the momentum conservation equation because pressure simply transfers momentum within the plasma without creating or destroying it.

$$\frac{\partial}{\partial t}\left(nmv_i\right) + \frac{\partial}{\partial x_j}\left(nm(v_i v_j)\right) + \frac{\partial}{\partial x_j}\left(P_{ij}\right) = 0 \tag{1.10}$$

We now perform the chain rule on the terms with both n and v because in general both variables are time and space dependent.

$$
\begin{aligned}
&nm\frac{\partial v_i}{\partial t} + v_i\frac{\partial nm}{\partial t} + v_i\frac{\partial (nmv_j)}{\partial x_j} + nmv_j\frac{\partial (v_i)}{\partial x_j} + \frac{\partial}{\partial x_j}\left(P_{ij}\right) = 0 \\
\rightarrow &nm\frac{\partial v_i}{\partial t} + nmv_j\frac{\partial (nmv_i)}{\partial x_j} + v_i\left(\frac{\partial (nm)}{\partial t} + \frac{\partial (nmv_j)}{\partial x_j}\right) + \frac{\partial}{\partial x_j}\left(P_{ij}\right) = 0 \\
\rightarrow &nm\frac{\partial v_i}{\partial t} + nmv_j\frac{\partial v_i}{\partial x_j} + \frac{\partial}{\partial x_j}\left(P_{ij}\right) = 0
\end{aligned} \tag{1.11}
$$

The term in parentheses in the second equation above vanishes in accordance with the mass conservation equation (1.4). At this point, any external forces may simply be added to the RHS of equation (1.11) as they do not conserve momentum. Examples of the external forces could be gravity or the Lorentz force. Returning to vector notation, the hydrodynamic momentum equation takes on the more familiar form below.

$$
\begin{aligned}
nm\left(\frac{\partial \mathbf{v}}{\partial t} + (\mathbf{v}\cdot\nabla)\mathbf{v}\right) &= -\nabla\cdot\overline{\overline{P}} + \Sigma\mathbf{F}_{ext} \\
\rightarrow nm\frac{D\mathbf{v}}{Dt} &= -\nabla\cdot\overline{\overline{P}} + \Sigma\mathbf{F}_{ext}
\end{aligned} \tag{1.12}
$$

In the final step, we have defined the advective derivative $D/Dt \equiv \partial/\partial t + \mathbf{v}\cdot\nabla$. The advective derivative accounts for changes in a variable due to explicit time variations (first term) as well as spatial variations resulting from following a fluid element (second term). This derivative is common throughout hydrodynamics.

Equations (1.4) and (1.12) are the foundation of hydrodynamics and determine the large-scale bulk motions of a dynamic plasma in the fluid limit. In order for the fluid limit to be valid, allowing for the use of the hydrodynamic equations, the plasma must satisfy certain conditions. Parker [1] provides a simple explanation of these conditions. First, consider the bulk motions of a certain plasma to have

length scale L which is divided into smaller lengths of size l, as in a finite differencing scheme [1]. In order for that scheme to yield satisfactory solutions to equations (1.4) and (1.12) above, the length scales must satisfy the relation $l \ll L$. At the same time, each cell of length l must be large enough so as to contain enough particles to give a statistically meaningful number density n. These coupled conditions on L, l, and n determine scenarios where plasmas may be treated as fluids. Fortunately, these conditions are routinely satisfied in many regions of interest throughout the solar system and galaxy making the fluid treatment of a plasma useful in many fields of physics and astrophysics.

1.2 Magnetohydrodynamics

By definition a plasma is at least partially ionized which means electric and magnetic forces must be included in the external forces of equation (1.12). Charged particles and their dynamics also alter those same fields necessitating the inclusion of Maxwell's equations. When the Lorentz force and Maxwell's equations are added to those of hydrodynamics, to account for the effects of electromagnetic forces and fields, we enter the field of magnetohydrodynamics (hereinafter MHD). This powerful combination is the perfect tool for describing the bulk motions of ionized gases throughout the galaxy. Recall the general form of the Lorentz force and Maxwell's equations in Gaussian units.

$$\mathbf{F}_L = q\mathbf{E} + \frac{1}{c} q\mathbf{u} \times \mathbf{B} \tag{1.13}$$

$$\nabla \cdot \mathbf{B} = 0 \tag{1.14}$$

$$\nabla \cdot \mathbf{E} = 4\pi\rho \tag{1.15}$$

$$\nabla \times \mathbf{B} = \frac{4\pi}{c}\mathbf{j} + \frac{1}{c}\frac{\partial \mathbf{E}}{\partial t} \tag{1.16}$$

$$\nabla \times \mathbf{E} = -\frac{1}{c}\frac{\partial \mathbf{B}}{\partial t} \tag{1.17}$$

These equations contain the variables for the magnetic field **B**, electric field **E**, particle velocity **u**, and electric current **j**. The combination of the hydrodynamic equations, Maxwell's equations and the Lorentz force actually over-constrains the system, however, and only two of these variables are necessary for our solution. Two logical pairs to consider are either **v** and **B** or **j** and **E**. Different scientific fields choose to work in one paradigm or the other as they were considered equivalent for years. While some still work in the **E-j** paradigm, Vasyliūnas [2] has shown that only **B** and **v** provide the correct physics in general. Once **v** and **B** are known, **j** and **E** are easily calculated.

$$\mathbf{j} = \frac{c}{4\pi}\nabla \times \mathbf{B} \tag{1.18}$$

$$\mathbf{E} = -\frac{1}{c}\mathbf{v} \times \mathbf{B} \tag{1.19}$$

These relations are the result of Maxwell's equations but the details of the derivation will be explained further in subsequent sections.

1.3 Single-fluid MHD

Including only the Lorentz force in the fluid momentum equation we arrive at the MHD specific momentum equation for a single plasma.

$$nm\left(\frac{\partial \mathbf{v}}{\partial t} + (\mathbf{v}\cdot\nabla)\mathbf{v}\right) = -\nabla\cdot\overline{\overline{P}} + nq\mathbf{E} + nq\frac{1}{c}\mathbf{v}\times\mathbf{B} + \Sigma\mathbf{F}_{ext} \tag{1.20}$$

Among the additional forces in $\Sigma\mathbf{F}_{ext}$, accounting for inter-particle collisions is possible. Collisions will be addressed in a later chapter, however, and will be neglected in the following section.

1.3.1 Ideal MHD

Though the fluid equations and Maxwell's equations describe the general motion of any electrically charged fluid we choose to focus on the specific case of a collisionless plasma, a limit that is actually realized quite often in interstellar plasmas. In a collisionless plasma, interactions with magnetic irregularities lead to particle scattering and isotropy, rather than interactions with other particles. Without any interparticle collisions, the less massive electrons in a plasma are able to easily move throughout the plasma resulting in very high electrical conductivity. A consequence of the high conductivity of the electrons is that a plasma is unable to maintain any substantial electric field in its own moving (with non-relativistic velocity $\mathbf{v}$) frame of reference; $\mathbf{E}' = 0$. Any imposed charge separation is easily neutralized by the mobile electrons. If we choose to move from the plasma frame to another observer's frame (perhaps at rest relative to the plasma) the electric and magnetic field undergo a Lorentz transformation. In the non-relativistic limit, this transformation has the following general form.

$$\mathbf{B} = \mathbf{B}' + \frac{1}{c}\mathbf{v} \times \mathbf{E}' \tag{1.21}$$

$$\mathbf{E} = \mathbf{E}' - \frac{1}{c}\mathbf{v} \times \mathbf{B}' \tag{1.22}$$

Primed variables denote the moving reference frame and unframed variables denote the observer's rest frame. As stated above, a collisionless plasma cannot support a electric field in its own frame so $\mathbf{E}' = 0$. The Lorentz transformations then simplify to the following.

$$\mathbf{B} = \mathbf{B}' \tag{1.23}$$

$$\mathbf{E} = -\frac{1}{c}\mathbf{v} \times \mathbf{B} \tag{1.24}$$

In this non-relativistic approximation, Ampére's law also simplifies by excluding the displacement current, $(1/c)\partial\mathbf{E}/\partial t$, which is now proportional to v/c using the transformations above. Substitution of equation (1.24) into Faraday's law leads to the magnetic induction equation of ideal MHD. Note that the magnetic field is the same in any frame of reference in the non-relativistic limit. The definitions of $\mathbf{j}$ and $\mathbf{E}$ in equations (1.18) and (1.19) are also now obvious in the same limit.

$$\frac{\partial \mathbf{B}}{\partial t} = \nabla \times (\mathbf{v} \times \mathbf{B}) \tag{1.25}$$

The induction equation provides a means to determine the time evolution of the magnetic field. In the case of ideal MHD the induction equation shows that the magnetic field is deformed by the motion of the plasma moving at velocity $\mathbf{v}$. This is because the magnetic field line are considered frozen into the highly conducting plasma. The lack of collisions also means there is no mechanism to dissipate the magnetic field so the field lines are only deformed and not destroyed. To see this result, begin with the definition of flux through a given surface $\mathbf{A}$ defined within the fluid.

$$\Phi = \oint \mathbf{B} \cdot d\mathbf{A} \tag{1.26}$$

If the magnetic field is carried along with the magnetic field, the magnetic flux through the surface **A** should be constant.

$$\frac{\partial \Phi}{\partial t} = \frac{\partial}{\partial t}\int_A \mathbf{B}\cdot d\mathbf{A} = \int_A \frac{\partial \mathbf{B}}{\partial l}\cdot d\mathbf{A} + \int_A \mathbf{B}\cdot\frac{\partial (d\mathbf{A})}{\partial t} \tag{1.27}$$

The rate at which the surface A (moving with the fluid) changes size is given by the cross product $\mathbf{v}\times d\mathbf{l}$ where $d\mathbf{l}$ is the path around $d\mathbf{A}$. This relation and the induction equation are now substituted into the flux equation.

$$\begin{aligned}&\int_A (\nabla\times(\mathbf{v}\times\mathbf{B}))\cdot d\mathbf{A} + \int_L \mathbf{B}\cdot(\mathbf{v}\times d\mathbf{l})\\ &\int_A (\nabla\times(\mathbf{v}\times\mathbf{B}))\cdot d\mathbf{A} - \int_A (\nabla\times(\mathbf{v}\times\mathbf{B}))\cdot d\mathbf{A} = 0\end{aligned} \tag{1.28}$$

The final step involves reordering the terms in the vector operations of the final term and applying Stoke's theorem to the integral. This result shows that the magnetic flux through the surface A does not change with time, equivalent to stating the field lines are frozen into the plasma.

We now have the equations necessary to describe ideal MHD, namely the fluid momentum equation and magnetic induction equation.

$$\rho\left(\frac{\partial \mathbf{v}}{\partial t} + \mathbf{v}\cdot\nabla\mathbf{v}\right) = -\nabla\cdot\overline{\overline{P}} + \frac{1}{4\pi}\nabla\times(\nabla\times\mathbf{B}) \tag{1.29}$$

$$\frac{\partial \mathbf{B}}{\partial t} = \nabla\times(\mathbf{v}\times\mathbf{B}) \tag{1.30}$$

1.3.2 Alfvén Waves

A simple result of ideal MHD is that of Alfvén waves, a phenomenon whereby magnetic perturbations travel along magnetic field lines just as perturbations travel along a string. To begin, we consider a stationary plasma threaded by a uniform magnetic field, $\mathbf{B_0}$, aligned along the $\hat{z}$ direction with uniform pressure. If we now perturb the uniform field and stationary plasma in the $\hat{x}$ direction (perpendicular to the original field) with variations in the $\hat{z}$ direction the momentum and induction equations are as follows.

$$\rho \frac{\partial v_x}{\partial t} = \frac{1}{4\pi} \frac{\partial^2 \delta B_x}{\partial z^2} \tag{1.31}$$

$$\frac{\partial \delta B_x}{\partial t} = -B_0 \frac{\partial \delta v_x}{\partial z} \tag{1.32}$$

The shear perturbations assumed here do not compress the fluid and $\nabla \cdot \overline{\overline{P}} = 0$. Using one equation to eliminate δv_x in favor of δB_x from the other we arrive at the single equation describing the behavior of the magnetic field perturbations.

$$\frac{\partial^2 \delta B_x}{\partial t^2} = -\frac{B_0^2}{4\pi\rho} \frac{\partial^2 \delta B_x}{\partial z^2} \tag{1.33}$$

This differential equation is easily recognized as a wave equation. Small perturbations in the magnetic field propogate along the field lines and travel at the Alfvén speed, $v_A = B_0/(4\pi\rho)^{1/2}$. Alfvén waves are present throughout the universe and provide one technique for probing magnetic field strength and particle density.

Had the plasma initially been non-stationary and traveling along the field lines in the $\hat{z}$ direction with speed v_0 the waves will simply be Doppler-shifted, $v_a + v_0$. This perturbation method will be applied and extended to more complicated problems in subsequent chapters.

1.4 Multi-fluid MHD

The single-fluid description of MHD can be extended to an arbitrary number of fluids of different particle species. In multi-fluid MHD, each species of particles are treated as separate plasmas subject to separate equations of motion. These equations may be coupled by common forces or collisions, but each species behaves in response to momentum individual equations. The different species may be as simple as a single population of ions and electrons or made to include multiple species of either, as well as neutral atoms. Multiples cases will be examined in this dissertation.

To arrive at the equations of ideal MHD, an implicit assumption was made with regards to the relative masses of electrons and protons; $m_e \ll m_p$. This assumption neglects the inertia of the electrons making the velocity of the proton plasma the bulk plasma velocity, $\mathbf{v}$. In this section, we will begin with separate momentum equations for ions (taken to be protons) and electrons.

$$n_i m_i \left(\frac{\partial \mathbf{v_i}}{\partial t} + (\mathbf{v_i} \cdot \nabla)\mathbf{v_i} \right) = -\nabla \cdot \overline{\overline{P}}_i + n_i q \mathbf{E} + n_i q \frac{1}{c} \mathbf{v_i} \times \mathbf{B} \tag{1.34}$$

$$n_e m_e \left(\frac{\partial \mathbf{v_e}}{\partial t} + (\mathbf{v_e} \cdot \nabla)\mathbf{v_e} \right) = -\nabla \cdot \overline{\overline{P}}_e - n_e q \mathbf{E} + -n_e q \frac{1}{c} \mathbf{v_e} \times \mathbf{B} \tag{1.35}$$

These two equations must now be combined by performing the operation (1.34) + (1.35). Using methods similar to those in section 1.1.2 simplifies this process.

$$\begin{aligned} &\frac{\partial}{\partial t} \left(n_i m_i \langle u_{i,j} \rangle + n_e m_e \langle u_{e,j} \rangle \right) \\ &\quad + \frac{\partial}{\partial x_k} \left(n_i m_i \langle u_{i,j} u_{i,k} \rangle + n_e m_e \langle u_{e,j} u_{e,k} \rangle \right) = \frac{1}{nec} \mathbf{j} \times \mathbf{B} \end{aligned} \tag{1.36}$$

The first and second indices on each velocity u denote the particle species and vector component respectively. Moving forward, the following definitions are used:

$$\mathbf{v}_{cm} = \frac{n_i m_i \mathbf{v}_i + n_e m_e \mathbf{v}_e}{n_i m_i + n_e m_e} \tag{1.37}$$

$$\mathbf{w} = \mathbf{u} - \mathbf{v}_{cm} \tag{1.38}$$

$$\langle \mathbf{w} \rangle = \mathbf{v} - \mathbf{v}_{cm} \tag{1.39}$$

Equation (1.37) is simply the speed of the center of mass for the combined fluid. The purpose of equations (1.38) and (1.39) is to recast the random motions of the individual particles in terms of $\mathbf{v}_{cm}$ [3]. These equations still imply that $\langle \mathbf{u} \rangle = \mathbf{v}$. Applying these useful definitions lead to the following on the LHS of equation (1.36).

$$\begin{aligned} &\frac{\partial}{\partial t}\left(n_i m_i v_{i,j} + n_e m_e v_{e,j}\right) \\ &\quad + \frac{\partial}{\partial x_k}\left(n_i m_i \langle \left(v_{cm,j} + w_{i,j}\right)\left(v_{cm,k} + w_{i,k}\right)\rangle + n_e m_e \langle \left(v_{cm,j} + w_{e,j}\right)\left(v_{cm,k} + w_{e,k}\right)\rangle\right) \end{aligned} \tag{1.40}$$

$$\begin{aligned} &\frac{\partial}{\partial t}\left(n_i m_i v_{i,j} + n_e m_e v_{e,j}\right) \\ &\quad + \frac{\partial}{\partial x_k}\Big[n_i m_i \left(\langle w_{i,j} w_{i,k}\rangle + v_{cm,j} v_{i,k} + v_{cm,k} v_{i,j} - v_{cm,j} v_{cm,k}\right) \\ &\quad + n_e m_e \left(\langle w_{e,j} w_{e,k}\rangle + v_{cm,j} v_{e,k} + v_{cm,k} v_{e,j} - v_{cm,j} v_{cm,k}\right)\Big] \end{aligned} \tag{1.41}$$

Once again, the $\langle w_j w_k \rangle$ terms are recognized as the pressure tensors due to the individual motions of ions and electrons, $\overline{\overline{P}}_i / n_i m_i$ and $\overline{\overline{P}}_e / n_e m_e$. Recall that these motions are now measured relative to $\mathbf{v}_{cm}$ rather than the bulk speed of the indi-

vidual species.

$$\begin{aligned}
&\frac{\partial}{\partial t}\left(n_i m_i v_{i,j} + n_e m_e v_{e,j}\right) \\
&\quad + \frac{\partial}{\partial x_k}\Big[P_{i,jk} + P_{e,jk} + v_{cm,j}\left(n_i m_i v_{i,k} + n_e m_e v_{e,k}\right) + v_{cm,k}\left(n_i m_i v_{i,j} + n_e m_e v_{e,j}\right) \\
&\quad - v_{cm,j} v_{cm,k}\left(n_i m_i + n_e m_e\right)\Big]
\end{aligned}$$

$$= \frac{\partial}{\partial t}\left(n_i m_i v_{i,j} + n_e m_e v_{e,j}\right) + \frac{\partial}{\partial x_k}\Big[P_{i,jk} + P_{e,jk} + \left(n_i m_i + n_e + m_e\right) v_{cm,j} v_{cm,k}\Big] \tag{1.42}$$

$$\rightarrow \frac{\partial}{\partial t}\left(\rho v_{cm,j}\right) + \frac{\partial}{\partial x_k}\left(\rho v_{cm,j} v_{cm,k} + P_{tot,jk}\right) = \frac{1}{nec}\mathbf{j} \times \mathbf{B} \tag{1.43}$$

In this expression, the total mass density is given by $\rho = n_i m_i + n_e m_e$ and the total pressure tensor by $\overline{\overline{P}}_{tot} = \overline{\overline{P}}_i + \overline{\overline{P}}_e$ defined as above. Conserving mass allows for a final simplification.

$$\rho \frac{\partial \mathbf{v}_{cm}}{\partial t} + \left(\mathbf{v}_{cm} \cdot \nabla\right)\mathbf{v}_{cm} = -\nabla \cdot \overline{\overline{P}}_{tot} + \frac{1}{c}\mathbf{j} \times \mathbf{B} \tag{1.44}$$

Equation (1.44) is the momentum equation for the combination of the fluid comprised of both the ions and electrons [4, 5].

Once multiple fluids are under consideration, a more formal treatment of the electric field is necessary. To proceed, once again consider the momentum equations for the ions and electrons. Calculating the difference $(q/m_i) * (1.34) - (q/m_e) * (1.35)$ leads to the following result with the new definition for the electric current $\mathbf{J} = n_i q \mathbf{v}_i - n_e q \mathbf{v}_e$.

$$\frac{\partial[q(n_i\mathbf{v}_i - n_e\mathbf{v}_e)]}{\partial t} + n_i q(\mathbf{v}_i \cdot \nabla)\mathbf{v}_i - n_e q(\mathbf{v}_e \cdot \nabla)\mathbf{v}_e \tag{1.45}$$
$$= -\frac{\nabla \cdot \overline{\overline{P}}_i}{m_i} + \frac{\nabla \cdot \overline{\overline{P}}_e}{m_e} + \left(\frac{n_i q^2}{m_i} + \frac{n_e q^2}{m_e}\right)\mathbf{E} + \left(\frac{n_i q^2}{m_i c}\mathbf{v}_i + \frac{n_e q^2}{m_e c}\mathbf{v}_e\right) \times \mathbf{B}$$

Continuing with the approximation $m_e \ll m_i$ any terms proportional to $1/m_i$ are neglected in the equation above. In the approximation of zero electron mass the electron velocity is not well defined so $\mathbf{v}_i$ is substituted for $\mathbf{v}_e$ using $\mathbf{J} = (c/4\pi)\nabla \times \mathbf{B}$. Solving for the electric field, the result is known as the Generalized Ohm's Law.

$$\mathbf{E} = -\frac{1}{c}\mathbf{v}_{cm} \times \mathbf{B} + \frac{1}{4\pi n_e q}(\nabla \times \mathbf{B}) \times \mathbf{B} - \frac{1}{n_e e c}\nabla \cdot \overline{\overline{P}}_e + \frac{m_e}{n_e q^2}\frac{D\mathbf{J}}{Dt} + \eta\mathbf{J} \tag{1.46}$$

The first term on the RHS is the electric field due to Lorentz transformation into the center of mass frame of reference. The rest of the terms are the Hall term, electon pressure term, inertial term and resistive term, respectively. Each one represents electric fields due to various effects. The resistive term has been added to account for possible collisions between electrons and ions. Each term becomes non-negligible at different scales of interest.

In the limit of very large length scales and negligible electron mass, equation (1.46) reduces to the electric field of ideal MHD and the freezes the magnetic field into the ion plasma.

$$\mathbf{E} = -\frac{1}{c}\mathbf{v}_i \times \mathbf{B} \tag{1.47}$$

1.4.1 Hall MHD

Continuing in the limit of $m_e \ll m_i$ but now at smaller length scales, the Hall terms approaches the magnitude of the advection term.

$$\frac{\text{Advection}}{\text{Hall}} \sim \frac{v_i B}{L} \times \frac{4\pi n_e q L^2}{cB^2} = \frac{v_i \omega_{g,i} L}{v_A^2} \tag{1.48}$$

Here, L is the length scale associated with variations in the magnetic field and ω_{ci} is the ion cyclotron frequency. If v_i and v_A are assumed to be of similar magnitude, the Advection-Hall ratio reduces to the following.

$$\frac{\text{Advection}}{\text{Hall}} \sim \frac{\omega_{ci} L}{v_A} = \frac{\omega_{pi} L}{c} \tag{1.49}$$

The term ω_{pi} is the ion plasma frequency, the rate at which charge perturbations oscillate in a plasma. The ratio c/ω_{pi} is known as the ion inertial length. Once length scales of interest approach the ion inertial length, the Hall term in the generalized Ohm's law is comparable to the advection term and must be considered.

$$\mathbf{E} = -\frac{1}{c}\mathbf{v}_{cm} \times \mathbf{B} + \frac{1}{4\pi n_e q}(\nabla \times \mathbf{B}) \times \mathbf{B} \tag{1.50}$$

The induction equation now takes on a slightly more complicated form.

$$\frac{\partial \mathbf{B}}{\partial t} = \nabla \times (\mathbf{v}_i \times \mathbf{B}) - \frac{c}{4\pi n_e q} \nabla \times [(\nabla \times \mathbf{B}) \times \mathbf{B}] \tag{1.51}$$

The advection term on the RHS is easily recognized, but the effects of the second is not immediately apparent. To better understand the physics resulting from the Hall term, reexpress the induction equation in terms of the electron velocity.

$$\frac{\partial \mathbf{B}}{\partial t} = \nabla \times (\mathbf{v}_e \times \mathbf{B}) \tag{1.52}$$

Written in this form, it is obvious that the magnetic field is actually frozen-into the electron plasma instead of the ion plasma. The Hall term accounts for this by causing the magnetic field to slip through the ion fluid when the motions of the two fluid differ greatly. On small scales, these differences become apparent. On large scales where the motions of electrons and ions are indistinguishable the Hall term is not necessary and the ion frozen-in condition is satisfied.

This limit can be understood in terms of the ion inertial length discussed above. The ion inertial length is the distance a magnetic perturbation travels during a single ion gyro period. As long as the size of that perturbation is much longer than the ion inertial length, an ion can remain tied to the field line and satisfy the frozen-in condition. For perturbation scales smaller than λ_i the perturbations will propagate past an ion too quickly for the ion to remain tied to the field line and only the electrons (with a much smaller inertial length) remain frozen-in. This regime where the ion and electron motions decouple is where the Hall term in the induction equation becomes important and the analysis moves from ideal to Hall MHD. Now that the ions and electrons no longer follow the same field line the charges separate from one another resulting in the additional electric field in the induction equation. This explains the magnetic field slipping through the ion plasma at small scales.

This effect is typically ignored because many astrophysical events occur on scales much larger than the ion inertial length and the ion-electron decoupling becomes

unimportant. Below is a table with typical length scales in various regions of interest.

Characteristic Length and Time Scales			
	Solar Corona	Solar Wind	ISM
λ_d (cm)	10^{-1}	10^2	10^3
c/ω_{pi} (cm)	10^3	10^6	10^7
r_c (cm)	10	10^6	10^7
ω_p (rad/s)	10^7	10^3	10^3
ω_c (rad/s)	10^{-1}	10^{-1}	10^{-2}

All MHD regimes are valid on length scales larger than λ_d (Debye length) and r_c (cyclotron radius), as well as time scales longer than ω_p^{-1} (plasma frequency) and ω_c^{-1} (cyclotron frequency).

One important applicatition of Hall MHD is magnetic reconnection. Magnetic reconnection requires the merging of magnetic field lines in order to facilitate the acceleration of energetic particles. This is not possible in ideal MHD where magnetic field lines are frozen into the plasma. Reconnection is a phenomenon that takes place on very short length scales where the Hall term becomes comparable to the typical advection term.

1.4.2 Choice of coordinate frame and electric fields

The above discussion of the Hall effect in MHD has illustrated the potential for different reference frames resulting in different effects on the plasma or plasmas being studied. This consequence is not surprising considering the Lorentz transformation of the electric field when moving between frames moving relative to one another.

In the limit of non-relativistic plasma speeds these transformation equations are as above.

$$\mathbf{E}' = \mathbf{E} - \frac{1}{c}\mathbf{v} \times \mathbf{B} \tag{1.53}$$

$$\mathbf{B}' = \mathbf{B} + \frac{1}{c}\mathbf{v} \times \mathbf{E} \tag{1.54}$$

In this case, $\mathbf{v}$, is the relative velocity between two different reference frames. For example, the stationary laboratory frame and the frame of the plasma moving at velocity $\mathbf{v}$. As we have already discussed, the electric field, $\mathbf{E}$, goes to zero in the frame of the highly conductive electrons. The Lorentz transformation equations then reduce to the following.

$$\mathbf{E}' = -\frac{1}{c}\mathbf{v}_e \times \mathbf{B} \tag{1.55}$$

$$\mathbf{B}' = \mathbf{B} \tag{1.56}$$

The magnetic field in the frame moving relative to the electrons is unchanged and the electric field in the moving frame is due to the motion of the frame relative to the unchanged magnetic field. Extending this result to Ohm's law reveals that electrical conductivity must also be frame-dependent.

$$\mathbf{j} = \sigma\mathbf{E} \tag{1.57}$$

In the non-relativistic limit we are already considering, Galilean transformations between frames dictate that the electric current, $\mathbf{j} = n_i e\mathbf{v}_i - n_e e\mathbf{v}_e$, is independent

of reference frame. This means that if $\mathbf{E}$ changes when moving from one frame to another, the conductivity σ must also change for $\mathbf{j}$ to remain constant. This results in interesting consequences due to changes in reference frames and Chapter 2 will explore this further.

One way to interpret this frame-dependent conductivity is to consider the motion of the magnetic field lines relative to the moving frame. As we have already discussed, ideal MHD assumes the plasma under question is perfectly conducting. This assumption leads to the frozen-in condition of the magnetic field lines moving with the plasma. If the electrical conductivity is finite, the frozen-in condition is broken and the magnetic field appears to slip through the plasma.

CHAPTER 2

The Physics of Partially Ionized Gas with Applications to Processes in the Interstellar Medium

2.1 Introduction

Many plasmas of interest in space physics, including the very-local interstellar gas and solar atmosphere, are only slightly ionized and comprised mostly of neutral atoms with long collision mean free paths. MHD is still the preferred method for studying the dynamics of these partially ionized plasmas. While the practice of using MHD to study predominantly neutral gases is common, there is some confusion as to how the problem should be treated. This is typically over which coordinate frame is best for carrying out the calculations. This problem will be discussed below, where we address the recent controversy concerning the proper equations for describing the interaction of the local interstellar medium with the heliosphere (Baranov and Fahr [6] and Florinski and Zank [7]).

Another problem involving partially ionized plasmas is the persistence of the Kolmogorov turbulence cascade in interstellar space. Previous theoretical work [8] has shown that the Alfvén waves propagating through a partially ionized plasma should be damped on scales smaller than $\sim 10^{15}$ cm. Observations strongly suggest that the cascade continues to small scales despite the damping [9]. A possible explanation for this persistence will be proposed in Section 3 below.

2.2 Basic Equations

2.2.1 Momentum

In order to address the controversy discussed in [6] and [7] we will review the basic MHD equations applicable to the case of partially ionized plasmas. To do so we must consider at least three separate fluids; the neutral atoms, protons and electrons. All three fluids have their corresponding momentum equations [1].

$$n_n m_p \frac{d\mathbf{v}_n}{dt} = -\nabla p_n + \frac{n_n m_p(\mathbf{v}_p - \mathbf{v}_n)}{\tau_{n,p}} + \frac{n_n m_p(\mathbf{v}_e - \mathbf{v}_n)}{\tau_{n,e}} \tag{2.1}$$

$$nm_p \frac{d\mathbf{v}_p}{dt} = -\nabla p_p + ne\left(\mathbf{E} + \frac{1}{c}\mathbf{v}_p \times \mathbf{B}\right) - \frac{nm_p(\mathbf{v}_p - \mathbf{v}_n)}{\tau_{p,n}} - \frac{nm_p(\mathbf{v}_p - \mathbf{v}_e)}{\tau_{p,e}} \tag{2.2}$$

$$nm_e \frac{d\mathbf{v}_e}{dt} = -\nabla p_e - ne\left(\mathbf{E} + \frac{1}{c}\mathbf{v}_e \times \mathbf{B}\right) - \frac{nm_e(\mathbf{v}_e - \mathbf{v}_n)}{\tau_{e,n}} + \frac{nm_e(\mathbf{v}_p - \mathbf{v}_e)}{\tau_{e,p}} \tag{2.3}$$

In the above equations $\mathbf{v}$, $\mathbf{w}$ and $\mathbf{u}$ are the bulk velocities of the neutrals, protons and electrons respectively. The number density of the atoms is n_n and the number densities of the protons and electrons are both simply n where we have assumed the total fluid to be quasi-neutral. Parker assumes the condition $n \ll n_n$ in [1] but this is not necessary in general. For simplicity, we also assume that neutral atoms and protons have the same mass m_p. The electrons have mass $m_e \ll m_p$. The quantities p_n, p_p, p_e, $\tau_{j,k}$ are the pressures of each species and the average times between collisions particle species j and k.

2.2.2 Collisions

The calculation of the change in momentum due to particle collisions varies throughout the literature so we believe a short aside is warranted. In the above equations, the force exerted on a plasma due to particle collisions is written in a simple form. While concise, the details of the force are obscured. Here, we will use Newton's second law to calculate the force due to particle collisions: $\mathbf{F} = \Delta\mathbf{p}/\Delta t$. To begin the derivation, recall the final velocities of two particles interacting by way of a one dimensional elastic collision.

$$v_{j,f} = \frac{v_{j,0}(m_j - m_k) + 2m_k v_{k,0}}{m_j + m_k} \tag{2.4}$$

$$v_{k,f} = \frac{v_{k,0}(m_k - m_j) + 2m_j v_{j,0}}{m_j + m_k} \tag{2.5}$$

The change in momentum, $\Delta p_j = p_{j,f} - p_{j,0}$, for a single particle can then be calculated.

$$\begin{aligned}
\Delta p_j &= m_j(v_{j,f} - v_{j,0}) \\
&= m_j \left[\frac{v_{j,0}(m_j - m_k) + 2m_k v_{k,0}}{m_j + m_k} - v_{j,0} \right] \\
&= m_j \left[\frac{v_{j,0}(m_j - m_k) + 2m_k v_{k,0} - (m_j + m_k)v_{j,0}}{m_j + m_k} \right] \\
&= m_j \left[\frac{-2m_k v_{j,0} + 2m_k v_{k,0}}{m_j + m_k} \right] \\
&= [m_j(v_{k,0} - v_{j,0})] \left[\frac{2m_k}{m_j + m_k} \right]
\end{aligned} \tag{2.6}$$

The factor of 2 is typically ignored in the literature. The time between collisions Δt is simply the inverse of the collision frequency between single particles of species j and k, $\nu_{j,k}$. The frequency of collisions between a single particle j and a plasma of multiple particles j is simply $n_k \nu_{j,k}$. Combining these results we find the expression for the force density on a plasma of particles j due to collisions with a plasma of particles k.

$$\mathbf{F}_{col-j,k} = \frac{n_k \nu_{j,k} n_j m_j m_k (\mathbf{v_k} - \mathbf{v_j})}{(m_j + m_k)} \tag{2.7}$$

In the notation of equations (2.1)-(3.3), $\tau_{j,k} = (m_j + m_k)/(n_k m_k \nu_{j,k})$. This definition of $\tau_{j,k}$ is typical throughout the literature though the details behind the derivation are typically not covered. Confusion stems from the differing subscripts on τ in each equation. Collisions must conserve momentum within the entire system, so collision terms between two species must be present in the equations for each of those species. For example, consider the collision terms between neutral atoms and protons.

$$\frac{n_n m_p (\mathbf{v}_p - \mathbf{v}_n)}{\tau_{n,p}} \tag{2.8}$$

$$-\frac{n_p m_p (\mathbf{v}_p - \mathbf{v}_n)}{\tau_{p,n}} \tag{2.9}$$

The sum of these terms should be 0 in order to conserve momentum. Without the above explanation this cancellation is not always obvious and is the reason for this aside.

2.2.3 Magnetic Field Evolution

The evolution of the magnetic field is once again determined by the magnetic induction equation.

$$\frac{1}{c}\frac{\partial \mathbf{B}}{\partial t} = -\nabla \times \mathbf{E} \tag{2.10}$$

In section 1.4.2 we discussed the effects that the choice of coordinate frame has on the observed electric field in that frame. Not surprisingly, this effect appears again in the multi-fluid treatment of a partially ionized plasma where there are three relevant frames to consider, one corresponding to each particle species.

Recall the non-relativistic Lorentz transformation equations for electromagnetic fields between frames moving relative to one another at a velocity $\mathbf{V}$.

$$\mathbf{B}' = \mathbf{B} + \frac{1}{c}\mathbf{V} \times \mathbf{E} \tag{2.11}$$

$$\mathbf{E}' = \mathbf{E} - \frac{1}{c}\mathbf{V} \times \mathbf{B} \tag{2.12}$$

2.3 Effects of Coordinate Frame Choice

2.3.1 Momentum and Magnetic Field

The use of different coordinate frames to study partially ionized plasmas has been discussed previously by Baranov and Fahr [6] as well as Florinski and Zank [7]. Both papers address issues pertaining to physical effects associted with the choice of coordinate frame and illustrate the importance of deciding on a frame in which

to work. In general there are an infinite number of frames in which to work but in the case of a partially ionized plasma, there are four reasonable frames to consider first. These are the frames moving with either the bulk velocities of the center of mass, the neutral atoms, the protons or the electrons. Baranov and Fahr [6] point out that ideal MHD is not always a valid assumption when working in the center of mass coordinate frame. This is true because the magnetic field is not frozen into this frame in general (section 1.4.1), a primary assumption of ideal MHD. The slipping of the field lines through the center of mass frame introduces a number of effects which can be difficult to interpret. The complications that arise from working in the center of mass frame are real but we are free to choose the frame in which we work. Usually, if $n_n << n$, the most useful frame is the one moving with the bulk speed of the protons, $\mathbf{w}$.

Once again, in the limit of low pressure and negligible electron mass we solve (3.3) for $\mathbf{E}$ and find the previous result $\mathbf{E} = -(1/c)\mathbf{u} \times \mathbf{B}$. This results shows that the magnetic field is frozen into the frame moving with the electron bulk velocity. Therefore, in this frame, the magnetic evolution equation is that of ideal MHD and the magnetic field is simply advected with the electron fluid.

$$\frac{\partial \mathbf{B}}{\partial t} = \nabla \times (\mathbf{v}_e \times \mathbf{B}) \tag{2.13}$$

Even though the magnetic evolution equation is simple in this case, the limit of massless electrons complicates their motion. When we take $m_e \ll m_p$, the electron fluid simply serves the purpose to quickly neutralize any electric field that develops in the plasma so solving for the exact motion can be difficult. Instead we can take the proton velocity to be the fluid velocity by replacing $\mathbf{v}_e$ with $\mathbf{v}_p - (c/4\pi ne)\nabla \times \mathbf{B}$ (Ampére's law).

$$\frac{\partial \mathbf{B}}{\partial t} = \nabla \times (\mathbf{v}_p \times \mathbf{B}) - \frac{c}{4\pi n e} \nabla \times [(\nabla \times \mathbf{B}) \times \mathbf{B}] \tag{2.14}$$

In doing so we recover the results of section 1.4.1 which introduces a Hall term, the second term on the right hand side, to the magnetic evolution equation. In section 1.4.1 we compared the magnitudes of the convection and the Hall terms and found the Hall term is only significant if $r_g/L \gtrsim 1$ or $v_a/L \gtrsim \omega_g$. Here r_g and ω_g are the proton gyro radius and frequency, v_a is the Alfvén speed and L is the scale over which $\mathbf{B}$ changes. For low energy particles and large astronomical distances the effect of the Hall term is negligible and the magnetic field is approximately frozen into the proton fluid.

Continuing in the limit of $m_e \ll m_p$ we substitute the electric field $\mathbf{E}$ into the proton momentum equation (2.3). Note that collision terms including electrons $\to 0$ in this limit as well.

$$nM \frac{d\mathbf{v}_p}{dt} = \frac{1}{4\pi} (\nabla \times \mathbf{B}) \times \mathbf{B} + \frac{nM(\mathbf{v}_p - \mathbf{v}_n)}{\tau_{p,n}} \tag{2.15}$$

Collisions between the protons and neutrals couple the neutrals to the proton fluid. The equation of motion for the neutrals (2.1) must then be included to close equations (2.14) and (2.15). This system of equations (valid while following the proton fluid) will be studied further in a subsequent section.

2.3.2 The Electrical Conductivity

Another interesting aspect of the coordinate frame ambiguity is the frame dependence of the electrical conductivity, σ. In resistive MHD, a difference in electrical

conductivity between frames determines how the magnetic field diffuses between those frames. In order to illustrate the frame dependence of the conductivity, we consider a common version of Ohm's law, $\mathbf{j} = \sigma\mathbf{E}$, which is accurate under the conditions of MHD [3]. Here, $\mathbf{E}$ is the electric field transformed to the relevant frame (as in equation (2.12)) considered in the calculation. In previous sections we have already discussed how $\mathbf{E}$ changes between moving frames but in the non relativistic limit $\mathbf{j}$ is unchanged (Ampere's law).

$$\begin{aligned}\mathbf{j} &= ne(\mathbf{v}_p - \mathbf{v}_e) = ne((\mathbf{v}_p - \mathbf{V}) - (\mathbf{u}_e - \mathbf{V})) \\ &= ne(\mathbf{v}_p - \mathbf{v}_e + \mathbf{V} - \mathbf{V}) = ne(\mathbf{v}_p - \mathbf{v}_e)\end{aligned} \tag{2.16}$$

In order for the current to be constant between frames, the conductivity must change to compensate for the changing electric field. In the frames moving with the electrons, protons, and neutrals we have the following electric fields.

$$\mathbf{E}_e = 0 \tag{2.17}$$

$$\mathbf{E}_i = \frac{1}{nec}\mathbf{j} \times \mathbf{B} \tag{2.18}$$

$$\mathbf{E}_n = \frac{1}{nec}\mathbf{j} \times \mathbf{B} - \frac{\tau_{p,n} B^2 \sin\theta}{nMc^2} j\hat{\mathbf{n}} \tag{2.19}$$

The angle θ is the angle between the vectors $\mathbf{j}$ and $\mathbf{B}$. Note that the terms involving collisions with electrons are still neglected in the equations above. The direction of the unit vector $\hat{\mathbf{n}}$ is normal to the local magnetic field while also in the plane defined by $\mathbf{B}$ and $\mathbf{j}$. In terms of the current, $\hat{\mathbf{n}} = -\hat{j}_{||} \sin\theta + \hat{j}_{\perp} \cos\theta$ where the parallel and perpendicular directions are relative to the magnetic field. It should also be noted that the equation for $\mathbf{E}_n$ is valid in the limit, $N >> n$,

used by Parker [1] where the momentum of the ions is neglected relative to that of the neutral atoms. If we insert these expressions for the different electric fields into Ohm's law and take the dot product of both sides with the current we can solve for the conductivity in each frame. In both the proton and electron frames, we find the conductivity to approach infinity consistent with ideal MHD. In the case of the neutral frame we find the conductivity to be finite.

$$\sigma_n = \frac{nMc^2}{\tau_{p,n} B^2 \sin^2\theta} \tag{2.20}$$

If we were to move away from the limit of $m_e \ll m_p$ and include the effects from collisions with electrons we would find the following conductivity.

$$\sigma_n = \left[\frac{4\pi}{c^2}\eta + \frac{\tau_{p,n} B^2 \sin^2\theta}{nMc^2}\right]^{-1} \tag{2.21}$$

$$\eta = \frac{mc^2}{4\pi n e^2}\left[\frac{1}{\tau_{e,n}} + \frac{1}{\tau_{e,p}}\right] \tag{2.22}$$

The quantity η above is simply the Ohmic resistivity due to electron-proton or electron-neutral collisions. When considering the problem of partially ionized plasmas, Cowling [10], found a "genuine reduction in the conductivity normal to the magnetic field", an effect termed Cowling conductivity. In the limit of $N >> n$, Cowling's result simplifies to σ_n above with $\theta = \pi/2$, which is simply the inverse sum of the Ohmic and Pedersen resistivities. This calculation clearly illustrates that the Cowling conductivity is frame dependent and only relevant if one chooses to work in the neutral atom (also center of mass in this case) frame of reference. This specific choice of frame is not always explicit in the literature so the use of Cowling

conductivity is not clearly justified, leading to confusion. The resistive term in (2.19) is also partly responsible for the complexity of the magnetic evolution equation in [6] as pointed out by [7]. By working in the proton frame, the resistive term does not appear and the magnetic evolution equation simplifies to (2.14).

2.4 Application to the interstellar turbulence problem

Observations show that the interstellar medium is turbulent with an rms fluctuation in quantities such as the density or magnetic field of the same order as the mean [9]. The turbulence is well described by a Kolmogorov-like energy spectrum. The theory of Kolmogorov turbulence proposes that large scale turbulent eddies break down into smaller and smaller eddies. This "energy cascade" from large to small scales terminates when dissipation removes the cascading energy. The resulting energy spectrum $E(k)$ follows a scale dependent power law, $E(k) \sim k^{-5/3}$, where k is the wave number (inverse length) of the eddy. This energy cascade occurs from length scales on the order of tens of parsecs to scales of kilometers [9]. Recently, some authors have questioned the existence of the Kolmogorov cascade on small scales in the partially ionized interstellar plasma [8, 11]. They propose that the Kolmogorov turbulence will be damped at scales less than about 10^{-16} cm due to the interaction of protons with neutral atoms. We examine this theory below.

Using equations (2.1), (2.14), and (2.15) we can determine the propagation of Alfvén waves through a partially ionized plasma composed of neutral hydrogen atoms, protons, and electrons. To do so we will follow a similar procedure to the one in section 1.3.2. Just as with the analysis of the fully ionized plasma, we assume a uniform magnetic field (once again directed in the $\hat{z}$ direction) permeates an initially motionless partially ionized plasma. The magnetic field and fluid velocities are then perturbed perpendicular to the magnetic field by the values δB, δw, and δv in the $\hat{x}$ direction. These perturbations are assumed to be oscillating in nature, $\sim exp(ikz - i\omega t)$, and vary only in the z direction.

$$\mathbf{B} = \delta B * e^{ikz - i\omega t}\hat{x} + B_0\hat{z} \tag{2.23}$$

$$\mathbf{w} = \delta w * e^{ikz - i\omega t}\hat{x} \tag{2.24}$$

$$\mathbf{v} = \delta v * e^{ikz - i\omega t}\hat{x} \tag{2.25}$$

Inserting the assumed solutions above into (2.1), (2.14), and (2.15) and solving the system of equations for the unknown quantities δB, δw, and δv we find the following cubic dispersion relation for ω.

$$\omega^2 + \frac{i\omega}{\tau_{p,H}}\left(1 - \frac{1}{1 - \frac{iN}{n}\omega\tau_{p,H}}\right) = \frac{B_0^2 k^2}{4\pi n M} \tag{2.26}$$

The quantities $\tau_{p,H}$, N, n, B_0, and M are the proton-hydrogen collision period, hydrogen number density, proton number density, average magnetic field, and the mass of protons and hydrogen atoms (taken to be equal).

Analytic solutions are possible for cubic polynomials though the complexity of the coefficients in the dispersion relation lead to equally complex solutions. First we will investigate the dispersion relation in two extreme limits and examine the simple results. In these limiting cases this cubic dispersion relation reduces to a quadratic equation with far more tractable roots. In the high-collision limit of $\omega\tau_{p,H} << 1$ the collisions between protons and hydrogen atoms are frequent enough to bind the two fluids. The resulting dispersion relation describes Alfvén waves propagating though a fluid of total mass density $M(n+N)$, that of both the neutral atoms and protons.

$$\frac{\omega^2}{k^2} = \frac{B_0^2}{4\pi(n+N)M} \tag{2.27}$$

In the opposite collisionless limit, $\omega\tau_{p,h} >> 1$, the proton-hydrogen collisions are too infrequent to bind the two fluids. The result is Alfvén waves that propagate through only the proton fluid with no contribution from the neutral atoms.

$$\frac{\omega^2}{k^2} = \frac{B_0^2}{4\pi n M} \tag{2.28}$$

In the intermediate range of $\omega\tau_{p,H}$, the roots of the dispersion relation become complex resulting in damping of the waves. Equation (2.26) is cubic in ω for $\omega\tau_{p,H} \sim 1$, however, making an analytic expression for the damping difficult to find. If we work in the limit of $n/N << 1$, (2.26) becomes quadratic in ω and we find the damping rate $\gamma \sim 1/\tau_{p,H}$. The rate of the turbulent cascade is simply v_a/λ and for relevant parameters is somewhat larger than γ allowing the cascade to continue to small scales. This is possibly why the turbulent cascade is observed to continue to small scales [9]. While damping does occur, the rate is slow enough to allow for the turbulent cascade to continue. These results match those found originally by Kulsrud and Pearce [12] though by different means using somewhat different limits.

2.5 Conclusions

The MHD treatment of a partially ionized plasma is widely used, but has recently led to controversy in the astrophysical and heliospheric fields. As one would expect in this case, the details of the different methods are quite varied throughout the literature. The most commonly confused detail seems to be the choice of reference frame and the corresponding fluid velocity. As Baranov and Fahr [6] pointed out, the choice of frame can have drastic results on how the problem is solved and the final results. If the fluid velocity is taken to be that of the center of mass, additional terms must be added to the equations of ideal MHD to account for non-ideal effects. Florinski and Zank [7] argued that working with the center of mass bulk velocity was

an unnecessary constraint and instead recommended taking the proton bulk velocity to be the fluid velocity. Strictly speaking, ideal MHD is not valid when working with the proton velocity because of the additional Hall term in (2.14). Most situations in space physics that deal with partially ionized plasmas occur over large enough length scales, however, that the Hall contribution to the induction equation is negligible leading to ideal MHD.

We have presented a possible explanation for the persistence of the Kolmogorov cascade in a partially ionized plasma. Previous authors have proposed that the waves comprising the Kolmogorov turbulence spectrum should be damped due to collisions between protons and hydrogen atoms. Observations, however, contradict these theories and show the cascade to continue below the proton-H damping scale. An analysis of the damping and cascade rates in a partially ionized plasma show that the cascade rate is somewhat larger allowing it to persist to small scales, and not be damped.

CHAPTER 3

Dynamics of a Three-Component Plasma Including Streaming Cosmic Rays

3.1 Motivation

We examine the problem of a composite fluid made up of a single electron species and two distinct ion populations, each singly charged but with different masses and velocities. One of the ion populations will represent galactic cosmic rays (hereinafter GCR) accelerated at a shock propogating away from a supernova remnant (hereinafter SNR). These three fluids will initially be threaded by a weak uniform magnetic field. The purpose of this paper is to determine the evolution of the magnetic field in the event that one of the ion fluids (the GCRs) moves with a bulk velocity parallel to the background magnetic field. Previous authors have predicted that the bulk motions of the GCRs lead to an instability in the magnetic field causing substantial amplification of the background field. In the first study of this instability, Bell [13] followed a partial fluid approach to derive the dispersion relation for the non-resonant streaming instability. The GCRs were treated using a method from Krall and W. [14] that offered little obvious insight into the dynamics of the GCRs.

In this paper, I will treat the GCRs as a fluid in order to make their dynamics more obvious. If the GCR motions trigger an instability, I will identify the necessary conditions for this to occur and determine whether or not the conditions are possible in nature. Along with explicitly including the GCR dynamics by way of the MHD momentum equation, no approximations are made with regard to the GCR interactions with the background magnetic field. I will consider the case of infrequent collisions between individual particles, however. The long mean free path of

the GCRs ensures this is a valid approximation. The three fluid approach outlined in this paper reveals a new minimum threshold on the energy density of galactic cosmic rays that must be exceeded in order to excite a streaming instability. This threshold has not been explored previously and is simply assumed to be satisfied in all cases where the Bell instability is applied.

3.2 Introduction

Blast waves propagating out from SNRs are thought to be the source of most GCRs up to an energy of $\sim 10^{15}$ eV [15, 16, 17, 18, 19]. Because the observed GCR spectrum follows a power law with constant index up to this energy, diffusive shock acceleration (hereinafter DSA) is the most likely primary acceleration mechanism [20, 21, 22, 23, 24]. When considering acceleration at a SNR, DSA at a quasi-parallel shock can only account for energies up to $\sim 10^{14}$ eV using the observed interstellar magnetic field and maximum scattering rate [25]. The acceleration must be more rapid in order to reach the energies at the knee of $\sim 10^{15}$ eV. In the case of DSA, this means the particles must be bound to the shock more effectively by the magnetic field. One way to make the acceleration more rapid at a parallel shock is to increase the magnitude of the magnetic field. Observational evidence supports amplification of the magnetic field beyond that caused by the compression of the fluid at the shock [26].

In order to amplify the magnetic field at a parallel shock, Bell [13] suggested a magnetohydrodynamic (hereinafter MHD) fluid instability capable of amplifying a transverse perturbation upstream of the shock to $\delta B/B_0 \sim 100$, where B_0 is the magnitude of the original field. This cosmic ray current-driven instability (hereinafter CRCD) is triggered by GCRs streaming along the uniform background magnetic field. The GCR current produces a separate return current in the background plasma to maintain overall charge neutrality. The return current excites transverse turbulence in the upstream region. In this formulation the GCR dynamics are not

considered with their only purpose being to establish the streaming current. Their motion is assumed to be constant and unchanged by any interactions with the surround environment. This simplification is valid in some cases but not in general. The goal of this analysis is to account for the dynamics of the GCRs from the beginning without any assumptions. This allows for determining when GCR dynamics can be explicitly ignored, ultimately leading to a Bell-like instability.

Once established, the excited transverse component scatters high energy GCRs, limiting their motion away from the shock increasing their acceleration rate. Bell finds that the amplified field is adequate to accelerate GCRs up to, and possibly beyond, 10^{15} eV. Observations of supernova remnants [19] strongly support the existence of an amplified magnetic field of the required magnitude. Others have also worked in the kinetic regime to examine Bell's streaming instability. While some work supports the large increase in δB [27, 28, 29, 30, 31, 32, 33, 34], some find the amplification is only moderate $\delta B/B_0 \lesssim 10$ [35]. Fluid approaches to this problem are present in the literature, but assumptions are made regarding the interactions between the GCRs and magnetic field [36, 37], something avoided within this treatment. Riquelme and Spitkovsky [38] have proposed an additional instability caused by the *perpendicular* streaming of GCRs relative to the background field. This perpendicular current-driven instability (hereinafter PDCI) is actually triggered by the pre-amplified field generated by the CRCD. Additional work has also been carried out concerning kinetic instabilities related to self excited waves in shocks [39].

Another possibility to account for the observed acceleration of GCRs to 10^{15}eV is that much of the acceleration takes place where the shock is quasi-perpendicular, in which case no upstream magnetic-field amplification is necessary [23, 24]. In that case, the observed amplification of the magnetic field could be the result of preexisting upstream turbulence warping the shock front, leading to turbulent motions of the plasma behind the shock that amplify the magnetic field through a turbulent

dynamo process [40, 41].

In the present paper I will take a previously unexplored approach to the original MHD problem of streaming GCRs at a quasi-parallel shock and compare the results with those found previously. The approach outlined below follows the dynamics of three separate MHD fluids; the background ions, background electrons and GCRs. In this paper, I explicitly include and retain the dynamics of the GCRs, treated here as a MHD fluid, without any simplifying assumptions. Bell [13] immediately assumed the GCRs to be energetic enough to move freely along magnetic field without significant scattering. As mentioned above, this assumption is satisfied in many cases but not in general. For this reason, no initial assumptions are made about the GCRs to allow for any effects on the system as a whole. This method of treating the GCRs as an MHD fluid has not been done previously and in this case allows us to identify the conditions necessary to transition from a stable to unstable state. Specifically a minimum threshold for the the energy density of the GCRs is found to allow for Bell-like instabilities to develop.

3.3 Relevant Equations

In order to carry out our multi-fluid treatment of this problem, we will begin by considering the dynamics of the three separate fluids mentioned above. Two of these fluids comprise the background plasma of singly charged ions and electrons. The third fluid will be the GCRs, also singly charged ions. In order to preserve overall charge neutrality, the electron fluid will have the appropriate number density to neutralize the positive charge of the background ions and GCRs. Below are the MHD momentum equations describing each of the three fluids: the background ions, electrons and GCRs.

$$n_{bi}m_{bi}D_{bi}\mathbf{v}_{bi} = \frac{1}{c}n_{bi}e\mathbf{v}_{bi}\times\mathbf{B} + n_{bi}e\mathbf{E} \tag{3.1}$$

$$n_{cr}m_{cr}D_{cr}\mathbf{v}_{cr} = \frac{1}{c}n_{cr}e\mathbf{v}_{cr}\times\mathbf{B} + n_{cr}e\mathbf{E} \tag{3.2}$$

$$n_{e}m_{e}D_{e}\mathbf{v}_{e} = -\frac{1}{c}n_{e}e\mathbf{v}_{e}\times\mathbf{B} - n_{e}e\mathbf{E} \tag{3.3}$$

In the notation above, D_α is once again short hand for the total or convective derivative, $D_\alpha \equiv \partial/\partial t + \mathbf{v}_\alpha \cdot \nabla$. The subscript α can represent either bi, cr or e depending on the fluid under consideration. As mentioned above, the electrons must neutralize the electric charge of both positively charged fluids so we take $n_e = n_{bi} + n_{cr}$.

Just as we have done in the previous chapters, the magnetic induction equation (Faraday's law) is now added to the above momentum equations to account for the time evolution of the magnetic field.

$$\frac{\partial\mathbf{B}}{\partial t} = -c\nabla\times\mathbf{E} \tag{3.4}$$

In order to begin combining these four vector equations, we note that $m_e \ll m_{bi}$ and $m_e \ll m_{cr}$, and thus neglect terms proportional to m_e. In this limit, equation (3.3) reduces to the following.

$$\frac{1}{c}n_{e}e\mathbf{v}_{e}\times\mathbf{B} + n_{e}e\mathbf{E} = 0 \tag{3.5}$$

From this result, it is clear that the electric field takes on the simple form below.

$$\mathbf{E} = -\frac{1}{c}\mathbf{v}_e \times \mathbf{B} \tag{3.6}$$

This result shows that within the frame moving with the electrons at velocity $\mathbf{v}_e$, the electric field $\mathbf{E} = 0$. Physically, the massless electrons can easily move to cancel any imposed external electric field. Using this expression for $\mathbf{E}$ in the induction equation we find the following result.

$$\frac{\partial \mathbf{B}}{\partial t} = \nabla \times (\mathbf{v}_e \times \mathbf{B}) \tag{3.7}$$

This result has the effect of freezing the magnetic field into the electron fluid which carries the field lines bodily with the motion of the fluid. This fact is simply the result of neglecting the inertia of the less massive electrons.

Because the electrons simply serve to neutralize any applied electric field, their specific dynamics are not essential to the problem at hand. Instead we will focus on the dynamics of the more massive ions. We can use Ampère's law to recast $\mathbf{E}$ in terms of the bulk velocities of the two remaining ion fluids which contribute nearly all of the inertia to the system. From the non-relativistic form of Ampère's law $(\partial \mathbf{E}/\partial t)$, we know that $\mathbf{j} = n_{bi} e \mathbf{v}_{bi} + n_{cr} e \mathbf{v}_{cr} - n_e e \mathbf{v}_e = (c/4\pi)\nabla \times \mathbf{B}$. Solving for $\mathbf{v}_e$ and substituting the result into the equation for $\mathbf{E}$ we find the expression for the electric field in terms of the remaining ion velocities.

$$\mathbf{E} = -\frac{1}{c}\frac{n_{bi}}{n_e}\mathbf{v}_{bi} \times \mathbf{B} - \frac{1}{c}\frac{n_{cr}}{n_e}\mathbf{v}_{cr} \times \mathbf{B} + \frac{1}{4\pi n_e e}(\nabla \times \mathbf{B}) \times \mathbf{B} \tag{3.8}$$

Having re-solved for $\mathbf{E}$ in terms of the ion velocities we now substitute the above expression into the magnetic induction equation.

$$\begin{aligned}\frac{\partial \mathbf{B}}{\partial t} =& \nabla \times \left(\frac{n_{bi}}{n_e} \mathbf{v}_{bi} \times \mathbf{B} \right) + \nabla \times \left(\frac{n_{cr}}{n_e} \mathbf{v}_{cr} \times \mathbf{B} \right) \\ &+ \nabla \times \left[\frac{c}{4\pi n_e e} (\nabla \times \mathbf{B}) \times \mathbf{B} \right]\end{aligned} \tag{3.9}$$

This version of the induction equation shows that the magnetic field is not frozen into the ion fluids in general. This is not surprising as the dynamics of the electrons and ions are different in general. The final term on the RHS, known as the Hall term, prevents this and the field lines are partly carried with the ion fluids but also slip through them. The Hall electric field is caused by charge separation occurring due to charged particles traveling at different speeds in a magnetic field. In some cases, the Hall term can be neglected and the magnetic field can be approximated as being frozen into the ions. The Hall term becomes important when the scale of the irregularities in the magnetic field is on the order of any of the ions' gyro radius. In order to keep this work as general as possible, we retain the Hall term throughout.

Now that we have determined the appropriate electric field for the situation at hand, we may substitute equation (3.8) into equations (3.1) and (3.2) which describe the dynamics of the background ions and GCRs. After substitution we find the following.

$$\begin{aligned}n_{bi} m_{bi} D_{bi} \mathbf{v}_{bi} = & \frac{n_{bi} n_{cr}}{n_e} \frac{e}{c} (\mathbf{v}_{bi} - \mathbf{v}_{cr}) \times \mathbf{B} \\ &+ \frac{n_{bi}}{n_e} \frac{(\nabla \times \mathbf{B}) \times \mathbf{B}}{4\pi}\end{aligned} \tag{3.10}$$

$$n_{cr} m_{cr} D_{cr} \mathbf{v}_{cr} = -\frac{n_{bi} n_{cr}}{n_e} \frac{e}{c} (\mathbf{v}_{bi} - \mathbf{v}_{cr}) \times \mathbf{B} + \frac{n_{cr}}{n_e} \frac{(\nabla \times \mathbf{B}) \times \mathbf{B}}{4\pi} \tag{3.11}$$

Equations (3.9), (3.10), and (3.11) represent nine dynamical equations in nine unknowns, $\mathbf{v}_{bi}$, $\mathbf{v}_{cr}$, and $\mathbf{B}$.

We will now study the equations by perturbing the values of $\mathbf{v}_{bi}$, $\mathbf{v}_{cr}$, and $\mathbf{B}$ about predetermined initial values. In this case, we begin with a uniform magnetic field, B_0, directed along the $\hat{z}$ direction and the GCRs moving with a non-relativistic bulk speed, v_{cr0}, in the same direction. The background ions begin nearly at rest, with $v_{bi0} << v_{cr0}$. In order for this scenario to be true, the massless electrons must move with bulk speed $v_{e0} \approx (n_{cr}/n_e) v_{cr0}$ in the same direction as the GCRs. This is necessary for the initial condition of a uniform magnetic field which requires zero net current. To further simplify our analysis, the perturbations to these initial conditions will be circularly polarized in $\hat{x}$ and $\hat{y}$ and only depend on the z coordinate.

$$\begin{aligned} \delta_x &\sim exp(ikz - i\omega t) \\ \delta_y &\sim \pm i \delta_x \end{aligned} \tag{3.12}$$

The + and - in the $\pm$ sign indicate perturbations that are right hand and left hand circularly polarized, respectively. The choice of circularly polarized perturbations reduces the number of unknown values to just three: δv_{bix}, δv_{crx}, and B_{1x}. The vector quantities $\mathbf{B}$, $\mathbf{v}_{bi}$, and $\mathbf{v}_{cr}$ are listed below.

$$\mathbf{B} = \delta B_x exp(ikz - i\omega t)(\hat{x} \pm i\hat{y}) + B_0\hat{z} \tag{3.13}$$

$$\mathbf{v}_{bi} = \delta v_{bix} exp(ikz - i\omega t)(\hat{x} \pm i\hat{y}) \tag{3.14}$$

$$\mathbf{v}_{cr} = \delta v_{crx} exp(ikz - i\omega t)(\hat{x} \pm i\hat{y}) + v_{cr0}\hat{z} \tag{3.15}$$

If we substitute the above assumed solutions into equations (3.9)-(3.11) we find the following system of three equations in the three unknowns.

$$\left[\omega \pm \frac{n_{cr}}{n_e}\omega_{c,bi}\right] v_{bix} + \left[\pm\frac{n_{cr}}{n_e}\omega_{c,bi}\right] v_{crx} + \left[\pm\frac{n_{cr}}{n_e}\frac{e}{m_{bi}c}v_{cr0} + \frac{kB_0}{4\pi n_e m_{bi}}\right] B_{1x} = 0 \tag{3.16}$$

$$\left[\mp\frac{n_{bi}}{n_e}\omega_{c,cr}\right] v_{bix} + \left[\omega - \left(kv_{cr0} \mp \frac{n_{bi}}{n_e}\omega_{c,cr}\right)\right] v_{crx} + \left[\mp\frac{n_{bi}}{n_e}\frac{e}{m_{cr}c}v_{cr0} + \frac{kB_0}{4\pi n_e m_{cr}}\right] B_{1x} = 0 \tag{3.17}$$

$$\left[\frac{n_{bi}}{n_e}kB_0\right] v_{bix} + \left[\frac{n_{cr}}{n_e}kB_0\right] v_{crx} + \left[\omega - \left(\frac{n_{cr}}{n_e}kv_{cr0} \pm \frac{k^2 B_0 c}{4\pi n_e e}\right)\right] B_{1x} = 0 \tag{3.18}$$

The quantities $\omega_{c,bi}$ and $\omega_{c,cr}$ are the cyclotron frequencies of the background ions and GCRs respectively, defined below.

$$\omega_{c,bi} = \frac{eB_0}{m_{bi}c} \tag{3.19}$$

$$\omega_{c,cr} = \frac{eB_0}{m_{cr}c} \tag{3.20}$$

This system of equations can be represented as a single matrix equation $A \cdot x = 0$.

$$\begin{pmatrix} \omega - \alpha & \beta & \gamma \\ \delta & \omega - \sigma & \Sigma \\ \kappa & \chi & \omega - \lambda \end{pmatrix} \begin{pmatrix} \delta v_{bix} \\ \delta v_{crx} \\ \delta B_{1x} \end{pmatrix} = 0$$

The Greek variables in the coefficient matrix A can be read from equations above. A solution to the matrix equation exists if the determinant of $A = 0$. Calculating the determinant of A leads to the following cubic equation in the perturbation frequency ω.

$$\begin{aligned} &\omega^3 - (\alpha + \sigma + \lambda)\omega^2 \\ &\quad + [\alpha(\sigma + \lambda) + \sigma\lambda - \Sigma\chi - \beta\delta - \gamma\kappa]\omega \\ &\quad + [-\alpha(\sigma\lambda - \Sigma\chi) + \beta(\delta\lambda + \Sigma\kappa) + \gamma(\delta\chi + \kappa\sigma)] = 0 \end{aligned}$$

This cubic equation above is the plasma dispersion relation describing the characteristics of this particular system. The roots of the dispersion relation reveal the behavior of the plasma. If the roots are purely real, small perturbations will not lead to runaway instabilities. Complex roots, however, mean the system is unstable to small perturbations which can then grow, perhaps rapidly. In the following section we will study the nature of the roots and the conditions which can lead to instabilities in the magnetic field.

3.4 Numerical Solutions to the Dispersion Relation

Having laid out the theoretical basis for our work in the preceding sections, we now begin the analysis of the dispersion relation from equation (3.3). Analytic solutions for the roots of a cubic equation can be calculated, but due to the complexity of the coefficients in equation (3.3) the resulting solutions would be too complicated, obscuring any conclusions. We instead study the dispersion relation by calculating the roots numerically and determine whether they are real or complex [42].

In this paper, we are primarily concerned with the development of instabilities so we will only focus on conditions that lead to complex roots. The nature of the roots of a polynomial equation, whether real or complex, is easily determined by calculating the discriminant, D, of the coefficients. The discriminant of a cubic equation of the form $ax^3 + bx^2 + cx + d$ is shown below.

$$D = b^2c^2 - 4ac^3 - 4b^3d - 27a^2d^2 + 18abcd$$

If $D > 0$, all of the roots of the cubic are real and if $D < 0$ only one root is real and the other two are complex conjugates corresponding to growth and decay. Once the nature of a root is determined, the actual values of the complex roots are calculated according to the process outlined in Numerical Recipes [42].

3.4.1 Parameters

One purpose of this work is to try and compare the results of this paper directly with those of [13] who made a more restrictive approximation with respect to the GCR dynamics. The GCRs were assumed to be completely unmagnetized and free to move along the background magnetic field. No consideration was made for their interaction with the other particles or magnetic field and doing so ensured the

development of a magnetic instability. By choosing not to make any assumptions ahead of time, the results of this paper are extended to a wide range of GCR populations beyond just unmagnetized particles. To begin the comparison, the dispersion relation (equation (3.3)) is first evaluated for a set of background plasma and GCR parameters mirroring those used by Bell. Our results are then directly comparable with those of [13]. The parameters are listed below.

$$
\begin{aligned}
B_0 &= 3 \times 10^{-6} \text{ G} \\
n_{bi} &= 1 \text{ cm}^{-3} \\
v_A &= 6.6 \times 10^5 \text{ cm/s} \\
v_{cr0} &= 1 \times 10^9 \text{ cm/s} \\
n_{cr} &= 1.52 \times 10^{-11} \text{ cm}^{-3} \\
\gamma_{cr} &= 1.05 \times 10^6
\end{aligned}
$$

The variable γ_{cr} is an "effective" Lorentz factor due to the relativistic random motions of the GCRs (recall the bulk velocity $\mathbf{u}_{cr}$ is non-relativistic) and is equal to m_{cr}/m_{bi} where m_{cr} is the relativistic mass of the GCRs. The values for n_{cr} and γ_{cr} are not explicitly stated in [13] but the values implied in the paper can be found with the aid of the Bell variables r_{g1} and k_{max}, the gyro radius of the GCRs and wavenumber of maximum unstable growth rate of the magnetic field, respectively.

$$
\begin{aligned}
r_{g1} &= \frac{\gamma_{cr} m_{bi} c^2}{e B_0} \\
\rightarrow \gamma_{cr} &= \frac{e B_0 r_{g1}}{m_{i1} c^2}
\end{aligned}
$$

$$k_{max} = \frac{n_{i2} e v_{i20} B_0}{2 n_{i1} m_{bi} v_A^2 c}$$
$$\rightarrow n_{cr} = 2 \frac{n_{bi} m_{bi} v_A^2 c}{v_{cr} e B_0} k_{max}$$

Using these parameters for the background plasma and GCRs we can calculate the coefficients of the dispersion relation over a wide range of wavenumbers k. With the coefficients determined, the frequency at each value of k can be calculated and compared to the results of [13]. The wavenumber range over which we examine the dispersion relation is $10^{-2} < kr_{g1} < 10^5$ and identical to that in Figure 2 in [13]).

Bell's Figure 2 plots the real and imaginary (unstable) components of the complex roots found in the dispersion relation of [13]. In our Figure 3.1 we have plotted the roots of our dispersion relation (3.3) which are calculated over an identical range of wavenumber. The real and complex portions are scaled and plotted in the same manner.

Comparing the two plots we see very similar behavior near the peak of the imaginary component of the roots. In both cases, the imaginary portion of the root peaks near $kr_{g1} \sim 10^3$ and then quickly drops off. Our graph does not exhibit the same shallow tail for $kr_{g1} > 10^3$, however, and instead goes to zero. Once the imaginary component drops off, the behavior of the real components agree very well for $kr_{g1} > 10^3$. Below the value $kr_{g1} < 10^3$, the behavior of the real components once again disagree, though in both plots the imaginary component is much greater than the real component. In Figure 2 from [13], the slope of the imaginary components breaks near $kr_{g1} \sim 1$ while the imaginary slope in Figure 3.1 remains the same. One explanation for the difference between the plots for $krg1 < 1$ and $kr_{g1} > 10^3$ is that Bell considers three separate regimes when studying his dispersion relation. The boundaries of his regimes coincide with these vales of kr_{g1}. We have not specified any such boundaries in our study and have not made any approximations over this range of kr_{g1}.

In this section, we have used our fluid approach to confirm the existence of an instability with characteristics similar to those of the Bell instability using the same parameters as [13]. In the next section we will explore a wider parameter space to better understand the general conditions necessary for the instability to develop.

3.4.2 Necessary Conditions for an Instability

We will once again study the dispersion relation over the same range of wavenumbers but we will instead change the values of n_{cr} and γ_{cr} and explore their effect on the development of instabilities. As we have mentioned above, these variables are not explicitly dealt with in [13] and their values are not well known in the literature so we will vary their values in our calculations and discuss possible realistic values for the two. The parameters for the background plasma and bulk velocity of the GCRs are generally well accepted so they will remain constant throughout. In the event that a combination of n_{cr} and γ_{cr} triggers an instability we will find the wavenumber corresponding to the highest growth rate (k_{max}) and the growth rate itself (γ_{max}) and compare them to the values predicted in [13]. Analytically, the values of k_{max} and γ_{max} are given by the expressions below.

$$k_{max} = \frac{j_{cr} B_0}{2 n_{i1} m_p v_A^2 c}$$

$$\gamma_{max} = k_{max} v_A = \frac{j_{cr} B_0}{2 n_{i1} m_p v_A c}$$

The results of this analysis for the various combinations of n_{cr} and γ_{cr} are compiled in Figure 3.2 below. The various values of γ_{cr} are plotted along the x axis and n_{cr} along the y. The gray region represents combinations of γ_{cr} and n_{cr} that lead to an instability with characteristics similar to those in [13] and values in the white region

do not. The white diamond in the gray region corresponds to the combination used in Bell (2004). It is obvious from the plot that as long as the product of $\langle \gamma_{cr} n_{cr} \rangle \gtrsim 10^{-7}$ an instability with characteristics very similar to those of [13] is triggered. If the product falls below this threshold, however, no instability at all is observed. This leads to the question of whether or not $\langle \gamma_{cr} n_{cr} \rangle \gtrsim 10^{-7}$ is a condition that can be satisfied under realistic circumstances. Neither one of these parameters is well defined in the vicinity of a supernova blast wave so we will discuss methods for estimating their values.

First, we will consider the observed energy density of GCRs to make a rough estimate of $\gamma_{cr} n_{cr}$. Including the recent results from Voyager 1 [43] we find $\rho_{cr} \approx 1.3$ eV/cm^3. If we take this value to be the energy density averaged over some collection of GCRs we write the relation.

$$\rho_{cr} = \langle n_{cr} E_{cr} \rangle = \langle n_{cr} \gamma_{cr} m_{cr,0} c^2 \rangle$$

Here, γ_{cr} is once again the relativistic Lorentz factor for the GCRs and $m_{cr,0}$ is the rest mass of the GCRs which are taken to be protons. Because $m_{cr,0}$ and c are constants they can be removed from the average leaving us to solve for the average of the quantity $\langle \gamma_{cr} n_{cr} \rangle$.

$$\rho_{cr} = \langle \gamma_{cr} n_{cr} \rangle m_{cr,0} c^2$$

$$\rightarrow \langle \gamma_{cr} n_{cr} \rangle = \frac{\rho_{cr}}{m_{cr,0} c^2}$$

For the values of $\rho_{cr} = 1.3$ eV/cm^{-3} and $m_{cr,0} = 938$ MeV/c^2 we find $\langle \gamma_{cr} n_{cr} \rangle \sim 10^{-9}$ cm^{-3}. This value of $\langle \gamma_{cr} n_{cr} \rangle$ is two orders of magnitude too low to reach the threshold

we have found to excite an instability. The estimate for $\gamma_{cr} n_{cr}$ used here is almost certainly a lower bound as the energy density of GCRs would be enhanced near the site of acceleration. It is not obvious if the increase would be enough to reach the 10^{-7} increase, however. Below, we address the question of how much the GCR energy density may increase at a shock.

In order to estimate this increase we will consider this problem in the frame moving with shock. In this frame, the background plasma moves with bulk speed v_{cr}. The GCRs have no bulk speed and only move with their random relativistic velocities. We wish to estimate the collective contribution of these random motions to the GCR energy density. To do so, we estimate the particle distribution function, $f(x, p)$, for the GCRs using the free kinetic energy of the background plasma. The kinetic energy density flux of the background plasma provides an upper constraint on the enthalpy flux of the GCRs, placing a limit on their total energy density.

$$\frac{1}{2} n_{bi} m_{bi} v_{cr}^3 > \frac{5}{2} P_{cr} v_2$$

Here, P_{cr} and v_2 are the GCR pressure and the fluid velocity downstream of the shock ($v_2 = v_{cr}/4$). The GCR pressure is limited by this expression which ultimately leads to a limit on the distribution function as we show below.

$$P_{cr} < \frac{4}{5} n_{bi} m_{bi} v_{cr}^2$$

In order to calculate P_{cr} we consider a generic GCR momentum distribution function $f(p)$.

$$\begin{aligned} P_{cr} =& \frac{1}{3}\int 4\pi p^2 \frac{p}{m_{cr}} p f(p) dp \\ =& \frac{4\pi}{3}\int \frac{p^4}{m_{cr}} f(p) dp \end{aligned}$$

Here, we have assumed an isotropic distribution function. The theory of DSA predicts a momentum distribution $\sim p^{-4}$ for a strong shock so we choose the following form for $f(p)$.

$$f(p) = f_0 \left(\frac{p}{p_0}\right)^{-4}$$

In this expression, p_0 and f_0 are the minimum momentum of the GCRs and a proportionality constant, respectively. Note that m_{cr} in our expression for P_{cr} is the relativistic mass of the GCRs, $m_{cr} = \gamma_{cr} m_0$, where m_0 is the rest mass of the GCRs taken to be protons. The mass of the high energy GCRs then depends on their momentum.

$$m_{cr} = m_0 \left[1 + \left(\frac{p}{m_0 c}\right)^2\right]^{1/2}$$

Inserting this into the above expression for P_{cr} we find the following.

$$P_{cr} = \frac{4\pi}{3} \int \frac{p^4}{m_0 \left[1 + (p/m_0 c)^2\right]^{1/2}} f_0 \left(\frac{p}{p_0}\right)^{-4} dp$$
$$= \frac{4\pi f_0 p_0^4}{3 m_0} \int_{p_0}^{p_{max}} \left[1 + \left(\frac{p}{m_0 c}\right)^2\right]^{-1/2} dp$$

Upon integration we find the following expression for the pressure of the GCRs in terms of the minimum cosmic ray momentum. The purpose of this expression is to determine particle distribution function resulting in GCR energy density observed by Voyager. The GCR pressure, P_{cr}, is calculated in terms of the distribution function.

$$P_{cr} = \frac{4\pi c f_0 p_0^4}{3} log \left(\frac{\frac{p_{max}}{m_0 c} + \sqrt{1 + \left(\frac{p_{max}}{m_0 c}\right)^2}}{\frac{p_0}{m_0 c} + \sqrt{1 + \left(\frac{p_0}{m_0 c}\right)^2}} \right)$$

Recall the previous inequality $P_{cr} < (4/5) n_{bi} m_{bi} v_{cr}^2$ which leads to an upper limit on f_0, the constant of proportionality for the GCR distribution function.

$$f_0 < \frac{3 n_{bi} m_{bi} v_{cr}^2}{5\pi p_0^4 c} \left[log \left(\frac{\frac{p_{max}}{m_0 c} + \sqrt{1 + \left(\frac{p_{max}}{m_0 c}\right)^2}}{\frac{p_0}{m_0 c} + \sqrt{1 + \left(\frac{p_0}{m_0 c}\right)^2}} \right) \right]^{-1}$$

Now, we evaluate f_0 for the above background plasma parameters with $p_0 = 3.127 \times 10^7$ eV/c and $p_{max} = 1 \times 10^{15}$ eV/c. These values for p_0 and p_{max} correspond to particles with energies of 5×10^5 eV (particles moving at the shock speed) and

$1{\times}10^{15}$ eV (particles near the knee of the GCR spectrum). We find $f_0 < 3.297{\times}10^{-26}$ $(\mathrm{eV/c})^{-3}\mathrm{cm}^{-3}$. The distribution function then takes on the following form.

$$f(p) = \left(\alpha 3.152 \times 10^4\right) p^{-4} \left(\frac{\mathrm{eV}}{\mathrm{c}}\mathrm{cm}^{-3}\right)$$

The variable α has a value between 0 and 1 and represents the fraction of available kinetic energy available to the GCRs. With $\alpha = 0.2$ the value of $\langle \gamma_{cr} n_{cr} \rangle = 2.37 \times 10^{-4}$ cm$^{-}3$, well above the established threshold above.

To this point, we have neglected any spatial dependence of the GCR distribution function. The behavior of $f(p)$ upstream and downstream is once again determined by DSA. Downstream of a shock, $f(p)$ is uniform in space so the distribution function remains the same as equation (3.4.2). Upstream, however, the diffusion of GCRs ahead of the shock result in an exponential decrease in $f(p)$ in the upstream region; $f(x,p) \sim exp(-x * v_{cr}/\kappa)$ where κ is the diffusion coefficient in the upstream region and equal to $\lambda * w/3$ with λ and w the GCR mean free path and the particle speed. For approximation purposes we move to the limit of Bohm diffusion where λ is simply the GCR gyroradius, $r_{g,cr}$. The individual particles are also moving relativistically so the particle speed $w \approx c$ and we find the following expression for κ in terms of the particle momentum, p.

$$\kappa = \frac{pc^2}{3eB_0}$$

The final expression for the distribution function upstream of the shock in terms of both x and p is below.

$$f(x,p) = \left(\alpha 3.152 \times 10^4\right) p^{-4} \exp\left(\frac{-3 v_{cr} e B_0}{pc^2} x\right)$$

Now that $f(x,p)$ is determined up to the value of α (numerical results suggest that α can be as large as $10\% - 20\%$ at a parallel shock [44, 45, 46]) for the GCRs at the shock considered here, we integrate over p to calculate $\langle \gamma_{cr} n_{cr}(x) \rangle$ for comparison with our derived limit above. Recall that the variable $\langle \gamma_{cr} n_{cr}(x) \rangle$ is a measure of energy density due to the random relativistic motions of the GCRs. Physically, this can be interpreted as a measure of how much GCRs are affected by interactions with the surrounding environment, such as irregularities in the magnetic field. Higher energy particles with a larger Lorentz factor scatter less frequently and have the ability to stream more freely along magnetic field lines. This streaming is integral to the excitation of a Bell-like instability at a shock. In the event that the GCRs are not as energetic (low Lorentz factor) and scatter more often a larger number of particles are required to effect the same result.

$$\begin{aligned} \langle \gamma_{cr} n_{cr}(x) \rangle &= \int_{p_0}^{p_{max}} 4\pi p^2 \gamma_{cr}(p) f(x,p) dp \\ &= \alpha 3.96 \times 10^4 \int_{p_0}^{p_{max}} p^{-2} \left[1 + \left(\frac{p}{m_0 c}\right)^2\right]^{1/2} \\ &\qquad \times \exp\left(\frac{-3 v_{cr} e B_0}{pc^2} x\right) dp \end{aligned}$$

By leaving x as a variable in equation (3.4.2), we are able to determine how far upstream the streaming instability can be triggered. This expression cannot be evaluated analytically in general so we must calculate $\langle \gamma_{cr} n_{cr}(x) \rangle$ for various values of x individually. The results of this calculation are plotted in Figure 3.3. The value

of $\langle \gamma_{cr} n_{cr}(x) \rangle$ drops below our threshold of 10^{-7} cm^{-3} at a distance $x_{off} \approx 5e19$ cm (≈ 16 pc) upstream of the shock (with $\alpha = 0.2$). Once a parcel of upstream plasma advecting towards the shock is within 16 pc of the shock, the frozen-in magnetic field can be amplified until the parcel passes into the downstream region where $f(x,p)$ is uniform and the Bell instability is suppressed. The growth rate predicted by Bell depends on the number density of GCRs, so the rate grows as the plasma parcel approaches the shock. In the linear approximation applied in this paper the magnetic field grows exponentially with time, $\sim \exp(\gamma_{max} t)$. To account for the time dependence of γ_{max} the growth is instead $\sim \exp(\int \gamma_{max}(t) dt)$.

$$\delta B(t) = \delta B_0 \exp\left(\int_0^{x_{off}/v_{cr}} \frac{n_{cr}(t) e v_{cr} B_0}{2 n_{bi} m_{bi} v_A c} dt \right)$$

Below is the calculation for determining $n_{cr}(t)$.

$$\begin{aligned} n_{cr}(t) &= \int_{p_0}^{p_{max}} 4\pi\alpha p^2 f(t,p) dp \\ &= \left(4\pi\alpha 3.152 \times 10^4\right) \\ &\quad \times \int_{p_0}^{p_{max}} p^{-2} \exp\left(\frac{-3 v_{cr} e B_0 (x_{off} - v_{cr} t)}{p c^2} \right) dp \end{aligned}$$

We have substituted the variable x for t where $x = x_{off} - v_{cr} t$. Performing the integrations over t and p for $x_{off} = 16$ pc we find that the original perturbation δB_0 can be amplified to over 300 times the original value before reaching the shock. It should be noted that the *perturbation* is amplified and not the background field. For a reasonable perturbation in this linear framework, $\delta B/B \sim 100$, the amplification of the perturbed field will be only ~ 3 times that of the background field. The amplification of the magnetic field is possible but not necessarily to the degree implied by previous authors also working in the linear approximation.

In Figure 3.4 we examine the value of $\langle \gamma_{cr} n_{cr} \rangle$ as a function of p_{max}. As p_{max} increases from $10p_0$ to 1×10^{15} eV/c, $\langle \gamma_{cr} n_{cr} \rangle$ decreases quickly from ~ 5 cm^{-3} to 1.49×10^{-2} cm^{-3}. As the free kinetic energy excites GCRs of increasing energy, the average value of $\langle \gamma_{cr} n_{cr} \rangle$ rapidly decreases because while the particle energy increases $\sim p$ the particle density decreases as $\sim p^{-4}$ according to DSA. This result implies that the highest energy GCRs are not necessary to excite the Bell instability. In fact, as the DSA power law unfolds the value of $\langle \gamma_{cr} n_{cr} \rangle$ decreases back towards the instability threshold. This effect is not pronounced enough to halt the instability, however, as GCRs with energies beyond 1×10^{15} eV are not accelerated at SNRs. The fact that GCRs near the knee are not necessary for exciting the Bell instability supports the case that the Bell instability may operate at young SNR.

The shock speed is another variable that affects the viability of the Bell instability. Figure 3.5 plots both the value of $\langle \gamma_{cr} n_{cr} \rangle$ as a function of p_{max} and the required threshold of $\langle \gamma_{cr} n_{cr} \rangle$ to trigger an instability for three values of v_{cr}: $c/30$, $c/100$, and $100v_A$. As we have already discussed, a shock speed of $c/30$ is more than enough to exceed the resulting threshold to trigger an instability, which is clearly illustrated in the figure. A slower speed of $c/100$ is still fast enough to trigger the instability as well. The final case of $v_{cr} = 100v_A$, however, shows that there is indeed a minimum shock speed (greater than v_A for any combination of γ_{cr} and n_{cr}) required for the instability to set in. As the value of v_{cr} decreases over several orders of magnitude the value of the instability threshold unsurprisingly increases. The effect of decreasing v_{cr} on the incoming energy is quadratic, however, so the energy available to accelerate the GCRs drops quickly with decreasing v_{cr}. Eventually the two effects suppress the instability completely.

In previous papers, the magnitude of the GCR Lorentz factor was the primary constraint for triggering the streaming instability. It was necessary for the Lorentz factor to be high enough that the GCRs could be considered unmagnetized from the magnetic field and thus their motion was unaffected by the field. In our fluid

formulation of the problem, not only is the magnitude of the Lorentz factor crucial to the instability but also the number density of the GCRs. I have found that the product of the two determines a condition for triggering the streaming instability.

3.4.3 Center of Mass Formulation

A physical explanation for the Bell instability is that a Lorentz force $\sim j_{cr} \times B$ pushes radially outward on the background plasma surrounding a perturbed (circularly polarized) magnetic field line. The magnetic perturbations along the field line are then pulled further outward along with the pushed plasma increasing the size of the perturbation and amplifying the magnetic field.

The above interpretation of the Bell mechanism explains why the results found here differ from those previously found when we considered this problem by following the motion of the center of mass of the multiple fluids. In that approach the momentum equations for the GCRs and background ions were combined to describe a single composite fluid. The method of combining momentum equations to consider only the center of mass motion is common in MHD and was chosen as a way to simplify the analysis of a complicated problem. The primary simplification in this case being that there was no net Lorentz force on the composite fluid. Note that the inertia of the electrons was neglected in this case as well. Because the induction equation couples the evolution of the magnetic field to the motion of the composite fluid, the lack of a Lorentz force to deform the fluid means there is no mechanism for stretching field lines and amplifying the magnetic field.

If the momentum equations for the GCRs and background plasma remain separate, each fluid experiences an equal and opposite Lorentz force $\sim j_{cr} \times B$ driving the two plasmas apart. Each fluid is still partially tied to the magnetic field by the induction equation so as the two fluids moved apart, field lines will be stretched between the plasmas leading to an amplification of the field. Considering only the center of mass motion masks this diverging motion as well as the mechanism behind

the Bell instability.

3.5 Discussion and Conclusions

Here we have presented a new method to analyze the problem of GCRs streaming along a uniform magnetic field embedded in a nearly stationary thermal plasma. To make our work as complete and transparent as possible we have explicitly included the equations describing the dynamics of the GCRs which are treated as a MHD fluid. No a priori assumptions are made about the characteristics or motions of the GCRs. This allows for perturbations to the GCR motions to develop naturally and have an effect on the rest of the system. The similar process in [13], done by calculating the variable σ [14], was difficult to understand. While the details behind the calculation of σ are not clear, the value is set to 0 in the regime leading to the instability. It appears that $\sigma \rightarrow 0$ represents the limit of very energetic GCRs, whose motion is unaffected by magnetic field fluctuations. The exact conditions for moving to this limit are not discussed, a point I have tried to clarify in this paper. Rather than assuming that the GCRs are too energetic to have their motion affected by the magnetic field I allow their motion to evolve with the rest of the system which is possible in general. In the event the perturbations to the GCR motion become negligible, the three fluid approach presented here allows the system to reach that limit (similar to $\sigma \rightarrow 0$) naturally rather artificially imposing that limit from the beginning.

As I have shown above, allowing the system to evolve this way reveals a crucial threshold in GCR energy density that must be exceeded to trigger an instability. The critical result of this work, however, calls into question whether or not the physical parameters present at a supernova blast wave are always sufficient to reach the threshold found above. By examining the equations of motion over a wide parameter range describing the GCRs, I have found that the quantity $\gamma_{cr} n_{cr}$, a measure of GCR energy density, must exceed the value of 10^{-7} cm$^{-}3$ for an instability to develop at

a typical non-relativistic shock. Through a number of calculations I have worked to determine whether this threshold can be reached under realistic conditions at a supernova blast wave. Calculations of GCR energy density in the ISM place this value too low, though some enhancement at the acceleration site is to be expected. Assuming a substantial amount ($\sim 20\%$) of the free kinetic energy of the system, the energy density of GCRs is high enough such that $\langle \gamma_{cr} n_{cr} \rangle$ exceeds the required value of $\sim 10^{-7}$ cm^{-3}. In this case, the streaming instability is a viable mechanism for magnetic field amplification.

The results of this paper support those of [13] in that the non-resonant streaming instability is possible in the mathematical sense. The equations describing this system of a stationary plasma and streaming GCRs allow for the development of an instability with characteristics similar to that in [13] as long as the derived GCR energy density threshold is surpassed. We have shown that this is possible for a typical non-relativistic shock such as the one considered in [13]. This limit should be considered and verified, however, for any case where the streaming instability is to be used to amplify the magnetic field near a supernova blast wave. The conclusion of this paper implies that the observed amplification of magnetic fields at SNRs [19] may be due to the streaming of GCRs upstream of the shock wave. Even if conditions are favorable, amplification to the extent presented by Bell [13] is certainly not guaranteed, however. In situations when these conditions are not satisfied, other mechanisms such as the turbulent dynamo proposed by [40] may explain the amplification of the magnetic field. Particle acceleration to the knee would then occur at the perpendicular portions of the shock without need for the streaming instability.

This work was supported, in part, by NASA under grants NNX08AH55G and NNX10AF24G. JRJ is grateful to A. R. Bell and M. A. Lee for helpful discussions which improved this paper.

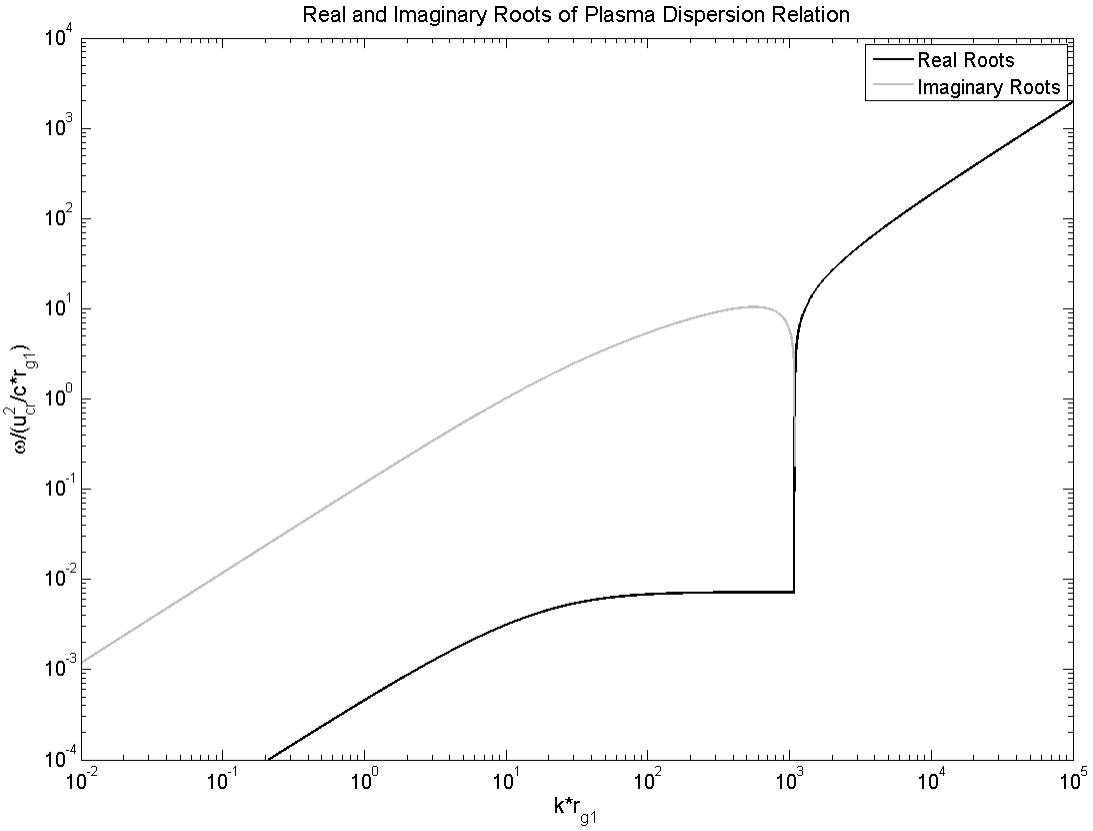

Figure 3.1: Numerical dispersion relation, Equation (3.3)

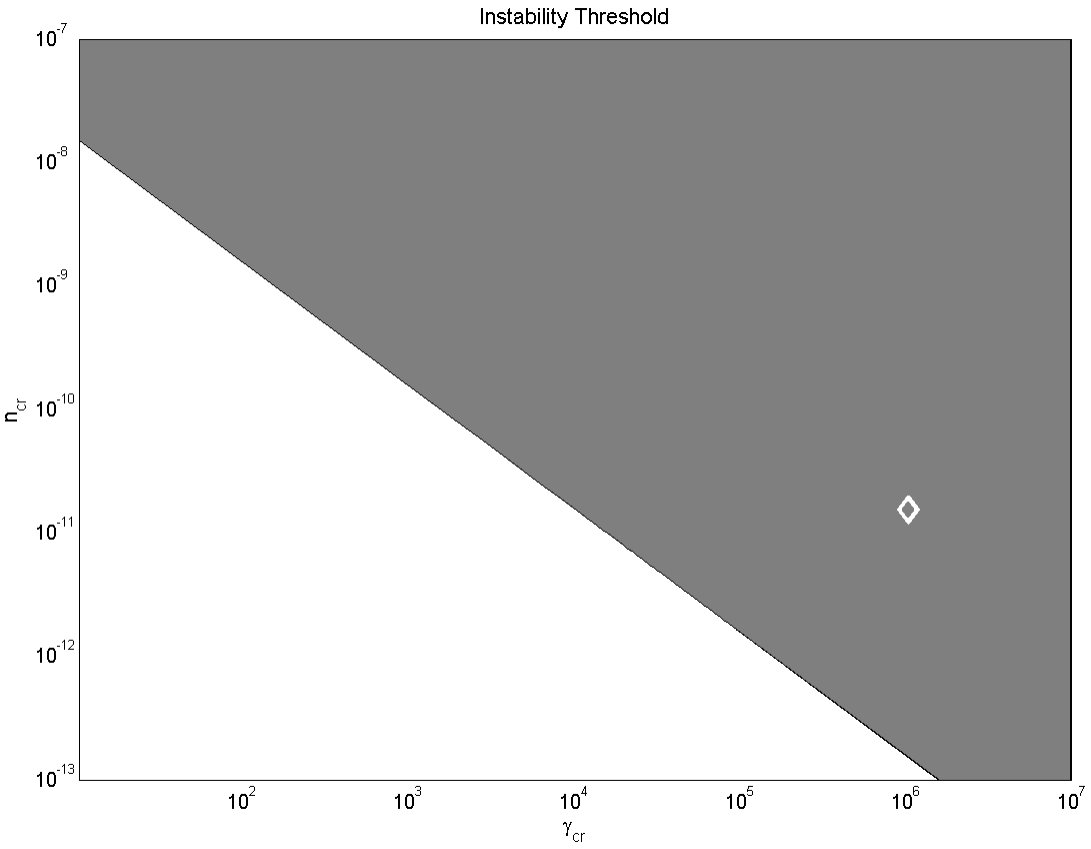

Figure 3.2: Conditions for instability to develop. Combinations of γ_{cr} and n_{cr} in the gray region lead to instability, combinations in the white region do not.

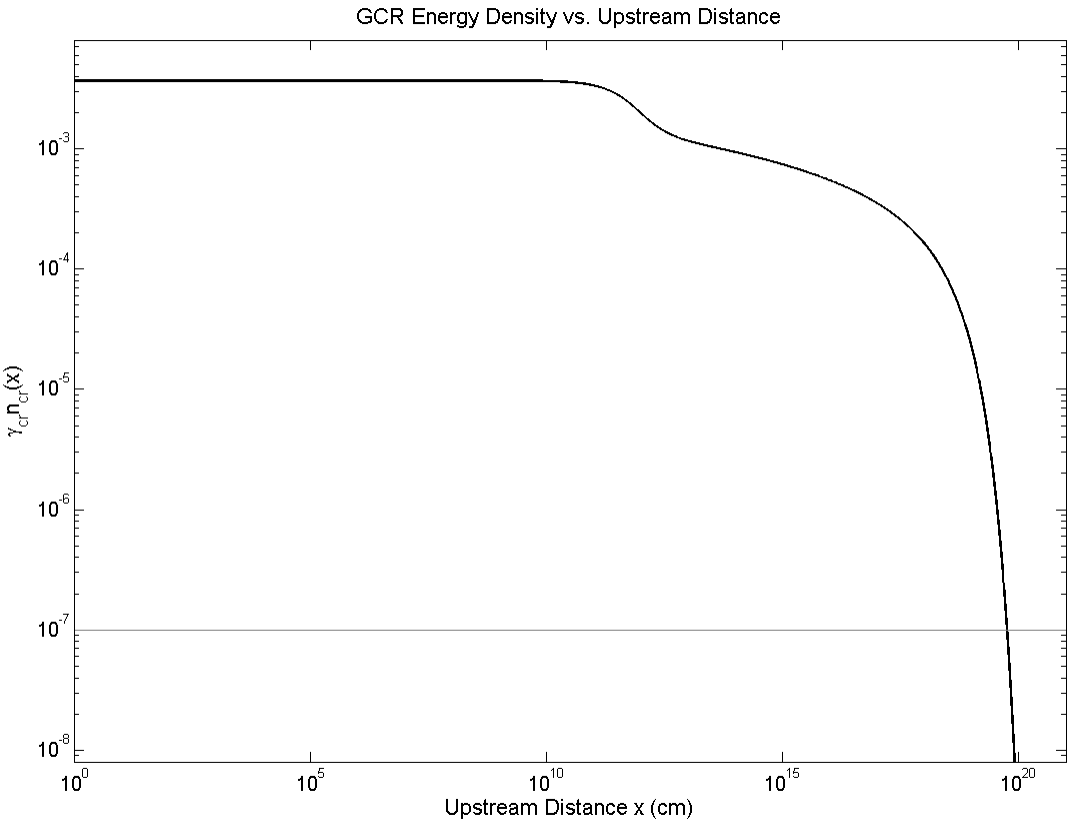

Figure 3.3: $\langle \gamma_{cr} n_{cr} \rangle$ vs. Upstream distance

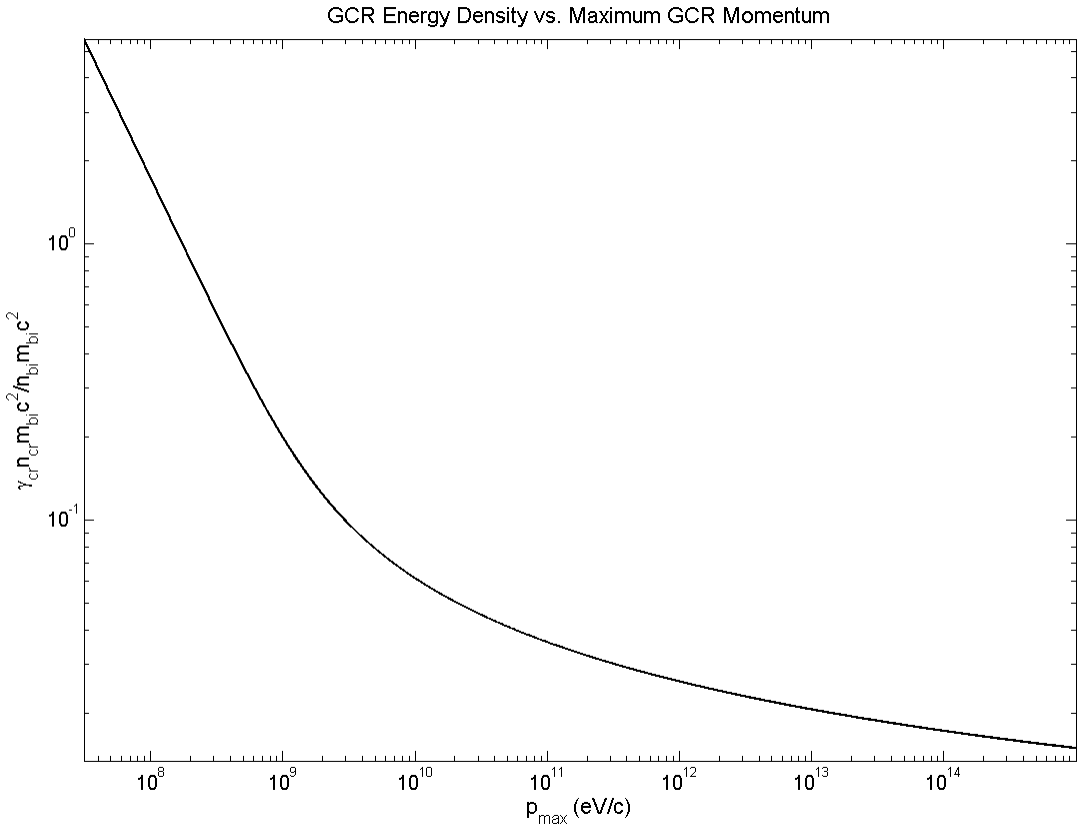

Figure 3.4: Effect of maximum GCR momentum on achieving instability threshold

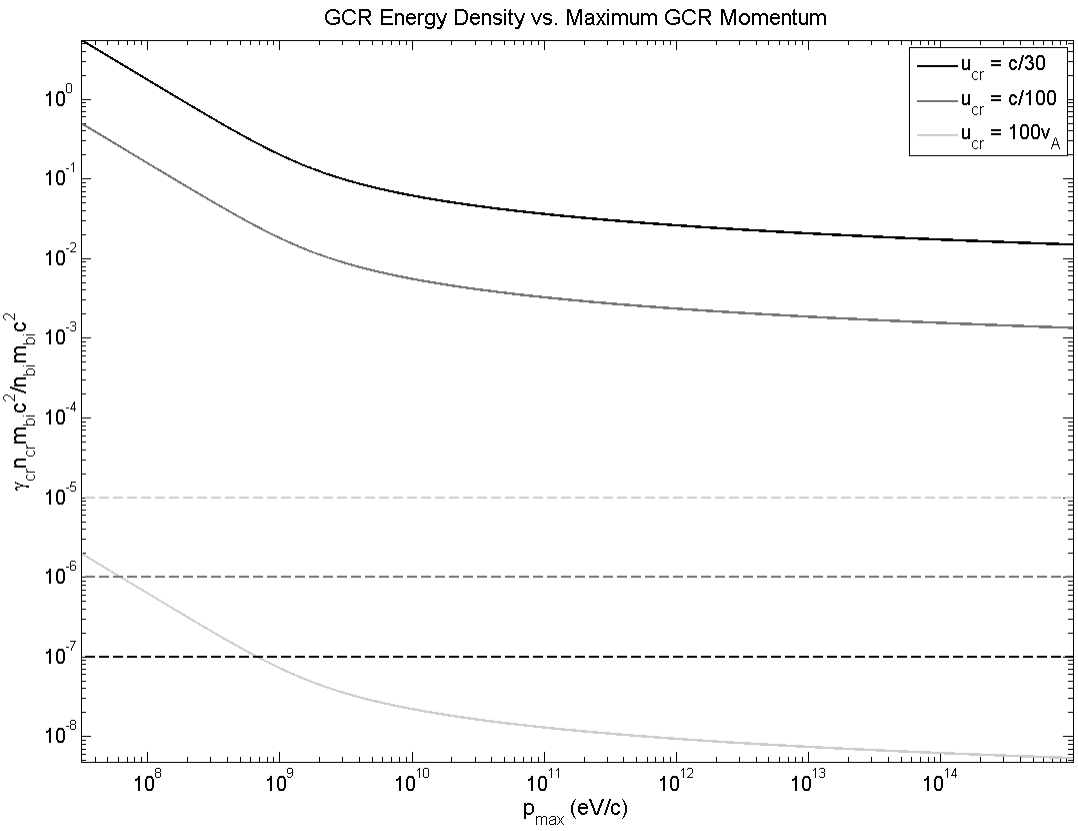

Figure 3.5: $\langle \gamma_{cr} n_{cr} \rangle$ vs. p_{max} for three different values of u_{cr} (solid lines) as well as the approximate necessary threshold to trigger the instabiliy (dashed lines).

REFERENCES

[1] E. N. Parker, *Conversations on Electric and Magnetic Fields in the Cosmos* (Princeton University Press, 2007).

[2] V. M. Vasyliūnas, GRL **28**, 2177 (2001).

[3] P. A. Sturrock, *Plasma Physics* (Cambridge University Press, 1994).

[4] T. J. Boyd and J. J. Sanderson, *Plasma Dynamics* (Cambridge University Press, 1969).

[5] T. J. Boyd and J. J. Sanderson, *The Physics of Plasmas* (Cambridge University Press, 2003).

[6] Baranov and Fahr, JGR **108**, 1110 (2003).

[7] V. Florinski and G. P. Zank, JGR **108**, 1438 (2003).

[8] J. C. Higdon, R. E. Lingenfelter, and R. E. Rothschild, APJ **698**, 350 (2009).

[9] J. W. Armstrong, B. J. Ricket, and S. R. Spangler, APJ **442**, 221 (1995).

[10] T. G. Cowling, *Magnetohydrodynamics* (Crane Russak & Co., 1976).

[11] Y. Lithwick and P. Goldreich, APJ **562**, 279 (2001).

[12] R. Kulsrud and W. P. Pearce, APJ **156**, 445 (1968).

[13] A. R. Bell, MNRAS **353**, 550 (2004).

[14] N. A. Krall and T. A. W., *Principles of Plasma Physics* (McGraw Hill, 1973).

[15] K. Koyama and et al., Nature **378**, 255 (1995).

[16] G. Allen and et al., APJ **487**, L97 (1997).

[17] T. Tanimori and et al., APJ **497**, L25 (1998).

[18] F. A. Aharonian, Astropart. Phys **11**, 225 (1999).

[19] E. G. Berezhko and et al., AAP **412**, L11 (2003).

[20] W. I. Axford and et al., Proc. 15th Int. Cosmic Ray Conf. **11**, 132 (1977).

[21] A. R. Bell, MNRAS **182**, 147 (1978).

[22] R. D. Blandford and J. P. Ostriker, APJ **221**, L29 (1978).

[23] J. R. Jokipii, APJ **255**, 716 (1982).

[24] J. R. Jokipii, APJ **313**, 842 (1987).

[25] P. O. Lagage and C. J. Cesarsky, AAP **125**, 249 (1983).

[26] J. Vink and J. M. Laming, APJ **584**, 758 (2003).

[27] B. Reville and et al, Plasma Phys. Control. Fusion **48**, 1741 (2006).

[28] P. Blasi and E. Amato, Proc. 30th Int. Cosmic Ray Conf. **2**, 235 (2008).

[29] E. Amato and P. Blasi, MNRAS **392**, 1591 (2009).

[30] A. R. Bell and et al., MNRAS **418**, 1208 (2011).

[31] B. Reville and et al., International Journal of Modern Physics D **17**, 1795 (2008).

[32] Y. Ohira and et al., APJ **698**, 445 (2009).

[33] E. Zweibel and J. Everett, APJ **709**, 1412 (2010).

[34] B. Reville and A. R. Bell, MNRAS **419**, 2433 (2012).

[35] M. A. Riquelme and A. Spitkovsky, APJ **694**, 626 (2009).

[36] A. Nekrasov and M. Sharmehri, APJ **756**, 77 (2012).

[37] A. Nekrasov and M. Sharmehri, APJ **788**, 47 (2014).

[38] M. A. Riquelme and A. Spitkovsky, APJ **717**, 1054 (2010).

[39] M. A. Lee, JGR **87**, 5063 (1983).

[40] J. Giacalone and J. R. Jokipii, APJ **663**, L41 (2007).

[41] A. Beresnyak and et al., APJ **707**, 1541 (2009).

[42] W. H. Press and et al., *Numerical Recipes in FORTRAN, 2nd Edition* (Cambridge University Press, 1992).

[43] E. C. Stone and et al., Science **341**, 150 (2013).

[44] D. C. Ellison and et al., APJ **453**, 873 (1995).

[45] J. Giacalone and et al., JGR **102**, 789 (1997).

[46] D. Caprioli and A. Spitkovsky, APJ **100**, 100 (2014).